

Cite as: T. C. Jones *et al.*, *Science*
10.1126/science.abi5273 (2021).

Estimating infectiousness throughout SARS-CoV-2 infection course

Terry C. Jones^{1,2,3†}, Guido Biele^{4,5†}, Barbara Mühlemann^{1,2}, Talitha Veith^{1,2}, Julia Schneider^{1,2}, Jörn Beheim-Schwarzbach¹, Tobias Bleicker¹, Julia Tesch¹, Marie Luisa Schmidt¹, Leif Erik Sander⁶, Florian Kurth^{6,7}, Peter Menzel⁸, Rolf Schwarzer⁸, Marta Zuchowski⁸, Jörg Hofmann⁸, Andi Krumbholz^{9,10}, Angela Stein⁸, Anke Edelmann⁸, Victor Max Corman^{1,2}, Christian Drosten^{1,2*}

¹Institute of Virology, Charité-Universitätsmedizin Berlin, corporate member of Freie Universität Berlin, Humboldt-Universität zu Berlin, and Berlin Institute of Health, 10117 Berlin, Germany. ²German Centre for Infection Research (DZIF), partner site Charité, 10117 Berlin, Germany. ³Centre for Pathogen Evolution, Department of Zoology, University of Cambridge, Cambridge CB2 3EJ, UK. ⁴Norwegian Institute of Public Health, 0473 Oslo, Norway. ⁵University of Oslo, 0315 Oslo, Norway. ⁶Department of Infectious Diseases and Respiratory Medicine, Charité-Universitätsmedizin Berlin, corporate member of Freie Universität Berlin and Humboldt-Universität zu Berlin, 10117 Berlin, Germany. ⁷Department of Tropical Medicine, Bernhard Nocht Institute for Tropical Medicine, and Department of Medicine I, University Medical Centre Hamburg-Eppendorf, 20359 Hamburg, Germany. ⁸Labor Berlin-Charité Vivantes GmbH, Sylter Straße 2, 13353 Berlin, Germany. ⁹Institute for Infection Medicine, Christian-Albrechts-Universität zu Kiel and University Medical Center Schleswig-Holstein, Campus Kiel, 24105 Kiel, Germany. ¹⁰Labor Dr. Krause und Kollegen MVZ GmbH, 24106 Kiel, Germany.

†These authors contributed equally to this work.

*Corresponding author. Email: christian.drosten@charite.de

Two elementary parameters for quantifying viral infection and shedding are viral load and whether samples yield a replicating virus isolate in cell culture. We examined 25,381 German SARS-CoV-2 cases, including 6110 from test centres attended by pre-symptomatic, asymptomatic, and mildly-symptomatic (PAMS) subjects, 9519 who were hospitalised, and 1533 B.1.1.7 lineage infections. The youngest had mean \log_{10} viral load 0.5 (or less) lower than older subjects and an estimated ~78% of the peak cell culture replication probability, due in part to smaller swab sizes and unlikely to be clinically relevant. Viral loads above 10^9 copies per swab were found in 8% of subjects, one-third of whom were PAMS, with mean age 37.6. We estimate 4.3 days from onset of shedding to peak viral load (8.1) and cell culture isolation probability (0.75). B.1.1.7 subjects had mean \log_{10} viral load 1.05 higher than non-B.1.1.7, with estimated cell culture replication probability 2.6 times higher.

Respiratory disease transmission is highly context dependent and difficult to quantify or predict at the individual level. This is especially the case when transmission from pre-symptomatic, asymptomatic, and mildly-symptomatic (PAMS) subjects is frequent, as with SARS-CoV-2 (1–8). Transmission is therefore typically inferred from population-level information and summarized as a single overall average, known as the basic reproductive number, R_0 . While R_0 is an essential and critical parameter for understanding and managing population-level disease dynamics, it is a resultant, downstream characterisation of transmission. With regard to SARS-CoV-2, many finer-grained upstream questions regarding infectiousness remain unresolved or unaddressed. Three categories of uncertainty are 1) differences in infectiousness among individuals or groups such as PAMS subjects, according to age, gender, vaccination status, etc., 2) timing and degree of peak infec-

tiousness, timing of loss of infectiousness, rates of infectiousness increase and decrease, and how these relate to onset of symptoms (when present), and 3) differences in infectiousness due to inherent properties of virus variants.

These interrelated issues can all be addressed via the combined study of two clinical virological parameters: the viral load (viral RNA concentration) in patient samples and virus isolation success in cell culture trials. While viral load and cell culture infectivity cannot be translated directly to in vivo infectiousness, and the impact of social context and behavior on transmission is very high, these quantifiable parameters can generally be expected to be those most closely associated with transmission likelihood. A strong relationship between SARS-CoV-2 viral load and transmission has been reported (9), comparing favorably with the situation with influenza virus, where the association is less clear (10, 11).

The emergence of more transmissible SARS-CoV-2 variants, such as the B.1.1.7 lineage (UK variant of concern, 202012/01), emphasizes the importance of correlates of shedding and transmission. The scarcity of viral load data in those with recent variants and PAMS subjects of all ages (12) is a blind spot of key importance because many outbreaks have clearly been triggered and fuelled by these subjects (2, 13–17). Viral load data from PAMS cases are rarely available, greatly reducing the number of studies with information from both symptomatic and PAMS subjects and that span the course of infections (12, 18). Making matters worse, it is not possible to place positive RT-PCR results from asymptomatic subjects in time relative to a non-existent day of symptom onset, so these cases cannot be included in studies focused on incubation period. Additionally, viral load time courses relative to the day of symptom onset rely on patient recall, a suboptimal measure subject to human error and which overlooks infections from pre-symptomatic or asymptomatic contacts (12). An alternative and more fundamental parameter, the day of peak viral load, can be estimated from dated viral load time series data, drawn from the entire period of viral load rise and fall and the full range of symptomatic statuses.

To better understand SARS-CoV-2 infectiousness we analyzed viral load, cell culture isolation, and genome sequencing data from a diagnostic laboratory in Berlin (Charité – Universitätsmedizin Berlin Institute of Virology and Labor Berlin). We first address a set of questions regarding infectiousness at the moment of disease detection, especially in PAMS subjects whose infections were detected at walk-in community test centres. Because these people are circulating in the general community prior to the detection of their infections, and are healthy enough to present at such centres, their prevalence and shedding are of key importance to the understanding and prevention of transmission. As well as PAMS subjects, we consider the infectiousness suggested by first-positive tests from hospitalised patients, and differences according to age, virus variant, and gender. A further set of temporal questions are then addressed by studying how infectiousness changes during the infection course. Using viral load measurements from patients with at least three RT-PCR tests, we estimate the onset of infectious viral shedding, peak viral load, and the rates of viral load increase and decline. Knowledge of these parameters enables fundamental comparisons between groups of subjects and between virus strains, and highlights the misleading impression created by viral loads from first-positive RT-PCR tests if the time of testing in the infection course is not considered.

Study composition

We examined 936,423 SARS-CoV-2 routine diagnostic RT-

PCR results from 415,935 subjects aged 0-100 years from February 24, 2020 to April 2, 2021. Samples were collected at test centres and medical practices mostly in and around Berlin, Germany, and analyzed with LightCycler 480 and cobas 6800/8800 systems from Roche. Of all tested subjects, 25,381 (6.1%) had at least one positive RT-PCR test (Table 1). Positive subjects had a mean age of 51.7 years with high standard deviation (sd) of 22.7 years, and a mean of 4.5 RT-PCR tests (sd 5.7), of which 1.7 (sd 1.4) were positive. Of the positive subjects, 4344 had tests on at least three days (with at least two tests positive), and were included in a time series analysis.

We divided the 25,381 positive subjects into three groups (Fig. 1). Hospitalised: 9519 (37.5%) subjects, includes all those who tested positive in an in-patient hospitalised context at any point in their infection; PAMS: 6110 (24.1%) subjects whose first positive sample was obtained in any of 24 Berlin COVID-19 walk-in community test centres, provided they were not in the Hospitalised category; and Other: 9752 (38.4%) subjects not in the first two categories (table S1). As Fig. 1 shows, there were very few elderly PAMS subjects, and relatively low numbers of young subjects in all three groups. The validity of the PAMS classification is supported by the fact that of the overall 6159 infections detected at walk-in test centres, only 49 (0.8%) subjects were later hospitalised. Subjects testing positive at these centres are almost certainly receiving their first positive test, because they are instructed to immediately self-isolate and our data confirms that such subjects are rarely re-tested: only 4.6% of people with at least three test results had their first test at a walk-in test center. Of the 9519 subjects who were ever hospitalised, 6835 were already in hospital at the time of their first positive test. PAMS subjects had a mean age of 38.0 years (sd 13.7), typically younger than Other subjects (mean 49.1 years, sd 23.5), with Hospitalised the oldest group (mean 63.2 years, sd 20.7). Typing RT-PCR indicated that 1533 subjects were infected with a strain belonging to the B.1.1.7 lineage, as confirmed by full genomes from next-generation sequencing (see materials and methods).

First-positive viral load

Across all subjects, the mean viral load (herein given as \log_{10} RNA copies per swab) in the first positive-testing sample was 6.39 (sd 1.83). PAMS subjects had viral loads higher than the Hospitalised for ages up to 70 years, as exemplified by a 6.9 mean for PAMS compared to a 6.0 mean in Hospitalised adult subjects of 20-65 years. Crude comparisons of viral loads in age groups show no substantial difference in first-positive viral load between groups of people aged over 20 years (Table 1), and that children and adolescents have mean first-positive viral loads differences ranging between -0.49 (-0.69, -0.29) and -0.16 (-0.31, -0.01) compared to

adults aged 20-65 (Table 2). Here and below, parameter differences between age groups show the younger value minus the older, so a negative difference indicates a lower value in the younger group. Ranges given in parentheses are 90% credible intervals.

We used a Bayesian thin-plate spline regression to estimate the relationship between age, clinical status, and viral load from the first positive RT-PCR of each subject, adjusting for gender, type of test center, and PCR system used. The Bayesian model well represents the observed data (Fig. 1B, Table 2, and fig. S1). The raw data and the Bayesian estimation (Fig. 2A), suggest considering subjects in three age categories: young (ages 0-20 years, grouped into five-year brackets), adult (20-65 years), and elderly (over 65 years). We estimated an average first-positive viral load of 6.40 (6.37, 6.42) for adults and a similar mean of 6.35 (6.32, 6.39) for the elderly (Fig. 2A). Younger age groups had lower mean viral loads than adults, with the difference falling steadily from -0.50 (-0.62, -0.37) for the very youngest (0-5 years) to -0.18 (-0.23, -0.12) for older adolescents (15-20 years) (Table 2). Young age groups of PAMS subjects have lower estimated viral loads than older PAMS subjects, with differences ranging from -0.18 (-0.29, -0.07) to -0.63 (-0.96, -0.32). Among Hospitalised subjects these differences are smaller, ranging from -0.18 (-0.45, 0.07) to -0.11 (-0.22, 0.01) (Table 2 and Fig. 2B). Viral loads of subjects younger than 65 years were around 0.75 higher for PAMS than for Hospitalised subjects (Fig. 2A), likely due to a systematic difference in RT-PCR test timing, discussed below.

Associating viral load with cell culture infectivity

We estimated the association between viral load and successful cell culture isolation probability (hereafter “culture probability”) by combining the Bayesian regression estimations with cell culture isolation data from our own laboratory (19) and from Perera *et al.* (20) (Fig. 2C). Across all ages, the average estimated culture probability at the time of first positive RT-PCR was 0.35 (0.01, 0.94). The mean culture probability is higher for PAMS cases, at 0.44 (0.01, 0.98), than Hospitalised cases, at 0.32 (0.00, 0.92) (Fig. 2D). Comparing PAMS cases, we found differences, in particular for children aged 0-5 compared to adults aged 20-65, with average culture probabilities of 0.329 (0.003, 0.950) and 0.441 (0.008, 0.981) respectively, and a difference of -0.112 (-0.279, -0.003). Age group differences in Hospitalised cases range from -0.028 (-0.104, 0.009) to -0.018 (-0.055, 0) (Table 2).

First-positive viral loads are weakly bimodally distributed (Figs. 1A and 2A), which is not reflected in age-specific means. The resultant distribution of culture probability includes a majority of subjects with relatively low, and a minority with very high culture probability (Fig. 2E and fig. S2). The highly-infectious subset includes 2228 of 25,381

positive subjects (8.78%) with a first-positive viral load of at least 9.0 \log_{10} , corresponding to an estimated culture probability of ~ 0.92 to 1.0. Of these 2228 subjects, 804 (36.09%) were PAMS at the time of testing, with a mean (median) age of 37.6 (34.0) and sd of 13.4 years. PAMS subjects are over-represented in this highly-infectious group among those aged 20-80 years, and Hospitalised subjects are over-represented in those aged 80-100 years (fig. S3).

Estimating B.1.1.7 infectiousness at first-positive test

The 1533 subjects infected with a B.1.1.7 virus in our dataset had an observed mean first-positive viral load of 7.38 (sd 1.54), which is 1.05 \log_{10} higher (0.97, 1.13) than non-B.1.1.7 subjects in the full dataset. To increase specificity, we compared 1453 B.1.1.7 cases with 977 non-B.1.1.7 cases using viral loads only from centres with B.1.1.7 and non-B.1.1.7 cases, and only from the same day or one day before or after the B.1.1.7 sample was taken. This analysis adjusted for clinical status, gender, RT-PCR system, subject age, and also modeled random test center effects. The results show that B.1.1.7 cases are associated with a 1.0 (0.9, 1.1) higher viral load (Fig. 3 and table S2). This results in a mean estimated B.1.1.7 subject culture probability of 0.50 (0.03, 0.97), considerably higher than the overall figure of 0.31 (0.00, 0.94) for the non-B.1.1.7 subjects in the comparison, corresponding to a median 2.6 (50% credible interval: 1.4, 5.1) times higher culture probability for samples from B.1.1.7 cases. To investigate whether there might be a difference in cell culture infectivity due to a factor other than viral load, we isolated virus from 105 samples (22 B.1.1.7, 83 B.1.177) in Caco-2 cells from a collection of 223 samples with matched viral loads. While no statistical difference was seen in the distribution of viral loads that resulted in successful isolation (fig. S4), uncertainty due to the routine diagnostic laboratory context, including uncontrolled pre-analytical parameters such as transportation time and temperature, together with the small isolation-positive sample sizes are insufficient to support a conclusion that the distributions do not differ (see materials and methods).

Estimating infectiousness over time

To investigate viral load over the course of the infection, we estimated the slopes of a model of linear increase and then decline of \log_{10} viral load using a Bayesian hierarchical model. The analysis used the time series of the 4344 subjects who had RT-PCR results on at least three days (with at least two tests being positive). The number of subjects with multiple test results skews heavily toward older subjects, with very few below the age of 20 meeting the criterium (Fig. 4A). We estimated time from onset of shedding to peak viral load of 4.31 (4.04, 4.60) days, mean peak viral load of 8.1 (8.0, 8.3), and mean decreasing viral load slope of -0.168

(-0.171, -0.165) \log_{10} per day (fig. S5). Figure S6 shows that while Hospitalised patients are estimated to be uniformly highly infectious at peak viral load, the infectiousness of PAMS subjects at peak load is more variable.

The temporal placement of the full 18,136 RT-PCR results from these 4344 subjects (80% of whom were hospitalised with COVID-19 at some point in their infections) is shown in fig. S7. Per-subject trajectories can differ considerably from that described by the mean parameters (Fig. 4B and fig. S8). Across all subjects, PAMS cases were on average detected 5.1 (4.5, 5.7) days after peak load, 2.4 (1.7, 3.0) days before non-PAMS cases, which were on average detected 7.4 (7.2, 7.6) days after peak load. We estimate that 962 (914, 1010) of the 4344 subjects (22.14% (21.04, 23.25)) had a first positive test before the time of their peak viral load, with a mean of 1.4 (1.3, 1.5) days before reaching peak viral load. Among the infections detected after peak viral load, the timing of the first positive RT-PCR test is estimated at 9.8 (9.6, 10.0) days after peak viral load, with sd of 6.9 (6.8, 7.0) days, reflecting a broad time range of infection detection. Estimated peak viral loads were higher in Hospitalised subjects than Other, and higher in Other than PAMS, with differences of 0.68 (0.83, 0.52) and 0.96 (0.33, 1.53) respectively (fig. S9 and table S3). No differences were seen according to gender. Viral load time courses are similar across age groups, though younger subjects have lower peak viral load than adults aged 45-55 (Fig. 5, A and C, fig. S10, and table S4). Model parameters suggest slightly longer time to peak, higher peak, and more rapid decline in viral load when the analysis is restricted to subjects with successively higher numbers of RT-PCR results (fig. S11 and table S5), with an increasing percentage of hospitalised subjects. Differences in model parameters according to the number of tests in subjects may reflect increased parameter accuracy due to additional data, though other factors associated with being tested more frequently may be responsible. The Bayesian estimation of the model agrees well with a separate second implementation based on simulated annealing (fig. S12, table S5, and supplementary text).

We estimate that the rise from near-zero to peak culture probability takes 1.8 (1.3, 2.6) days, with a mean peak culture probability of 0.74 (0.61, 0.85). Mean culture probability then declines to 0.52 (0.40, 0.64) at five days and to 0.29 (0.19, 0.40) at ten days after peak viral load. Subject-level time courses can deviate substantially from these mean estimates (Fig. 4C). Peak culture probabilities for age groups range from a low of 0.54 (0.39, 0.71) for 0-5 year olds to 0.80 (0.67, 0.90) for subjects over 65 years. The least infectious youngest children have 78% (61, 94) of the peak culture probability of adults aged 45 to 55 (Fig. 5, B and D, and table S4). Insufficient data precludes a reliable B.1.1.7 viral load time series analysis at this point.

Discussion

Limitations

Our analysis attempted to account for effects of gender, PCR system, and test center type. Although we could not incorporate inter-run variability or the variability in the sample pre-analytic, such as type of swab or initial sample volume in our conversion of RT-PCR cycle threshold values to \log_{10} viral load values, these variabilities apply to all age groups and do not affect the interpretation of data for the purpose of the present study. If the proportion of subjects with a certain clinical status differs between age groups in the study sample, this could lead to over- or underestimation of differences in viral load between age groups. However, as our study compares viral load between age groups stratified by clinical status, it appears unlikely that differential testing biases our results.

Interpreting first-positive viral loads

Viral loads and their differences are not easy to interpret, absent knowledge of when in the disease course the samples were taken and the correspondence between viral load and shedding. The higher first-positive viral loads in PAMS subjects than Hospitalised subjects are likely due to time of detection. This is suggested in the first place by the estimated 2.4 (1.7, 3.0) day difference in test timing, which would produce a viral load difference of ~ 0.4 using the -0.168 daily viral load decline gradient from the (mainly hospitalised) time series subjects. Additionally, the time series of PAMS, Other, and Hospitalised subjects estimates that, throughout the infection course, the Hospitalised group have higher viral loads than Other, who are in turn higher than PAMS (fig. S9 and table S3). This relationship holds across age groups (fig. S13) and also in a fine-grained split of test centres by clinical severity (fig. S14). Similarly, the lower first positive viral loads in elderly PAMS subjects may be due to these subjects being less likely to be tested as early due to being more likely to be house-bound, less likely to be employed, less mobile, more cautious and inclined to get tested with only mild symptoms, etc. The impact on infectiousness of differences in viral load must be informed by where the viral loads fall on the viral load / infectivity curve. In our data, the viral loads involved in the difference between the means in children and adults and the difference between means in B.1.1.7 and non-B.1.1.7 subjects result in quite different corresponding culture probabilities (see below).

A highly-infectious minority and over-dispersion

The bimodal distribution of culture probabilities (Fig. 2, D and E) shows a small group of 8.78% of highly-infectious subjects. This qualitatively agrees with a model (21) and a study (22) concluding that 10% and 15% of index cases, respectively, may be responsible for 80% of transmission. Oth-

er studies reported that 8-9% of individuals harboured 90% of total viral load (23), that in cases from India (24) and Hong Kong (6) ~70% of index cases had no secondary cases. The risk posed by PAMS subjects is highlighted by the fact that 36.1% of the highly-infectious subjects in our study were PAMS at the time of the detection of their infection, that their mean age was 37.6 years with a high standard deviation of 13.4 years (figs. S2 and S3), and our estimate that infectiousness peaks 1-3 days before onset of symptoms (if any).

Comparison with influenza virus

Absent direct knowledge from a large number of SARS-CoV-2 transmission events, we could try to draw conclusions regarding infectiousness from studies of other respiratory viruses, such as influenza. However, it has become clear that there are important differences and uncertainties that would cast doubt on such a comparison. Influenza may have later onset of viral shedding, shedding finishes earlier, there may be a lower secondary attack rate, viral loads are much lower, there is variation between virus subtypes, the role of asymptomatic subjects in transmission is uncertain or thought to be reduced, and the frequency of asymptomatic infections is uncertain, especially in children (10, 11, 25-29). Age-specific behavioral differences do however make a large contribution to the established higher shedding of children compared to adults in influenza. This should be an important consideration for SARS-CoV-2, as shown by studies indicating higher transmission between children of similar ages (6, 24) and high transmission heterogeneity (22). Despite many decades of close study of influenza virus, the relationship between viral load and transmission is unclear (10, 11). The situation with respiratory syncytial virus is even less clear (30). Understanding SARS-CoV-2 transmission will likely be at least as challenging, given the high frequency of transmission from PAMS subjects (1-8), suggesting an important role for clinical parameters, given the apparently strong association between viral load and transmission, independent of symptoms (9).

Estimated infectiousness in the young

The differences we observe in first-positive RT-PCR viral load between groups based on age are minor, as in other studies (31-35) and the viral loads in question, in the range of 5.9 to 6.6 (Table 1), are in a region of the viral load / culture probability association where changes in viral load have relatively little impact on estimated culture probability (Fig. 2C). Comparisons between adult viral loads and those of children and the relative infectious risks they pose are difficult due to the likely influence of non-viral factors. Nasopharyngeal swab samples, which often carry higher viral loads, are rarely taken from young children due to pain and

lack of cooperation, and the sample volume carried by smaller pediatric swab devices is lower than in larger swabs used for adults (36). Infections in mildly-symptomatic children may be initially missed and only detected later (37), resulting in lower first-positive viral loads. Our results of similar viral load trajectories for children and adults (Fig. 5), and the numeric range of the viral load values in question (Fig. 2C), suggest that viral load differences between children and adults are too small to alone produce large differences in infectiousness. The relative impact on transmission of general age-related physiological differences, such as different innate immune responses (38), may be small as compared to the impact of large differences in frequency of close contacts and transmission opportunities.

Timing of estimated peak infectiousness relative to onset of symptoms

We estimated the time from onset of shedding to peak viral load at 4.3 days. Previous studies and reviews of COVID-19 report mean incubation times of 4.8 to 6.7 days (4, 39-44), which suggests that, on average, a period of high infectivity can start several days before symptoms onset. Viral load rise may vary between individuals, and limitations of the available data suggest that our analysis may underestimate inter-individual variation in viral load increase. The failure to isolate virus in cell culture beyond 10 days from symptom onset (19, 20, 35, 45, 46) together with our estimated slope of viral load decline also suggests peak viral load occurs 1-3 days before symptom onset (supplementary text). Data from 171 hospitalised patients from a Charité - Universitätsmedizin cohort suggest a figure of 4.3 days (fig. S15 and supplementary text).

Estimated infectiousness of the B.1.1.7 variant

We found an approximately 1 log₁₀ higher first-positive viral load in people infected with a B.1.1.7 virus than people infected with a wild-type. The scale of the viral load difference and the fact that it is also present in the comparison between B.1.1.7 infected subjects and non-B.1.1.7 infected subjects drawn from the same test centres at the same times, argue that the difference is not due to a systematic difference in time of sampling. The 1 log₁₀ higher B.1.1.7 viral load can be compared to implied 5-10x higher B.1.1.7 viral loads in two large and closely-controlled UK studies, a vaccine trial (47) and a mortality study (48), based on RT-PCR cycle threshold differences of ~3 and 2.3 respectively. Several other studies also appear to point to a higher B.1.1.7 viral load (49-52) (supplementary text). Importantly, the mean B.1.1.7 viral load value in our study falls in a region of the viral load / culture probability curve with steep gradient (Fig. 2C), resulting in an estimated culture probability considerably higher than for non-B.1.1.7 subjects. Although a strong

correlation has been observed between SARS-CoV-2 viral load and transmission (9), here we are estimating infectivity probability from cell culture trials. Any impact of a change in viral load on transmission will be highly dependent on context, so the large difference in estimated culture probability in our data is only a proxy indication of potentially higher transmissibility of the B.1.1.7 strain. We estimate B.1.1.7 infected subjects having a 2.6 times higher mean culture probability than non-B.1.1.7 infected subjects. This range can be compared to a UK study that found a 1.3 relative increase in secondary attack rates for B.1.1.7 index cases in ~60,000 household contacts (53), a UK study estimating a 1.7 to 1.8 increase in transmission (54), and to an estimate of a 43% to 90% higher reproductive number (55).

Summary

Our results indicate that PAMS subjects in apparently-healthy groups can be expected to be as infectious as hospitalised patients at the time of detection. The relative levels of expected infectious virus shedding of PAMS subjects (including children) is of high importance because these people are circulating in the community and it is clear that they can trigger and fuel outbreaks (56). The results from our time series analysis, and their generally good agreement with results from studies based on other metrics (often epidemiological), show that accurate estimations can be directly obtained from two easily-measured virological parameters, viral load and sample cell culture infectivity. Such results can be put to many uses: to estimate transmission risk from different groups (by age, gender, clinical status, etc), quantify variance, show differences in virus variants, highlight and quantify over-dispersion, and to inform quarantine, containment, and elimination strategies. Our understanding of the timing and magnitude of change in viral load and infectiousness, including the impact of influencing factors, will continue to improve as data from large studies accumulate and are analyzed. A major ongoing challenge is to connect what we learn about estimated infectiousness from these clinical parameters to highly context-dependent in vivo transmission. Based on our estimates of infectiousness of PAMS subjects and the higher viral load found in subjects infected with the B.1.1.7 variant, we can safely assume that non-pharmaceutical interventions such as social distancing and mask wearing have been key in preventing many additional outbreaks. Such measures should be employed in all social settings and across all age groups, wherever the virus is present.

Materials and methods

Age ranges

Age categories for the analysis of the first-positive test results mentioned in the text indicate mathematically open-

closed ranges of years (e.g., 0-5 signifies (0-5] years). We group subjects up to 20 years old into age categories spanning five years, subjects from 20 to 65 years into an adult group, and elderly subjects into a 65+ category. This categorisation is motivated by the observed data and the Bayesian estimation of viral load differences between children of different ages and adults. The age groupings used in the viral load time series analysis are broader in the younger categories to increase the cardinality of those groups, due to the fact that few young people have at least three RT-PCR tests (Fig. 4A).

Viral loads

Viral load is semiquantitative, estimating RNA copies per entire swab sample, while only a fraction of the volume can reach the test tube. The quantification is based on a standard preparation tested in multiple diluted replicates to generate a standard curve and derive a formula upon which RT-PCR cycle threshold values are converted to viral loads. This approach does not reflect inter-run variability or the variability in the sample pre-analytic, such as type of swab or initial sample volume (varying between 2.0 and 4.3 mL). However, these variabilities apply to all age groups and do not affect the interpretation of data for the purpose of the present study.

Viral load figures are given as the logarithm base 10. Viral load is estimated from the cycle threshold (Ct) value using the empirical formulae $14.159 - (Ct * 0.297)$ for the Roche Light Cycler 480 system and $15.043 - (Ct * 0.296)$ for the Roche cobas 6800/8800 systems. The formulae are derived from testing standard curves and cannot be transferred to calculate viral load in other laboratory settings. Calibration of the systems and chemistries in actual use is required.

B.1.1.7 viral load analysis

No assignment regarding symptomatic status was made for B.1.1.7 subjects due to uncertainties regarding exact operational protocols at outbreak hospitals. B.1.1.7 assignment to samples was initially made according to typing-RT-PCR tests that detect the N501Y and 69/70 deletion in the amino acid sequence of the virus spike protein. Examination of the complete viral genome of 49 samples confirmed that the subjects were in fact infected with the B.1.1.7 variant, with all variant-defining substitutions and deletions (57) found in all cases. No consistent additional mutations or deletions/insertions were found in the sequences.

Sequencing read mapping was performed with Bowtie, with alignment using MAFFT, and visual inspection using Geneious Prime (all version numbers given below). For the statistical comparison of B.1.1.7 and non-B.1.1.7 subjects, we identified test centres (hospital departments or wards, or

organisations outside hospitals) that reported B.1.1.7 cases, and chose as comparison groups non-B.1.1.7 cases that were detected in these test centres on the same day or one day earlier or later. By modeling random effects for test centres, we estimate the expected viral load difference as the average of the within-test center differences. The consistent effect of B.1.1.7 throughout a range of comparison scenarios is shown in table S2.

Sample type

An estimated 3% of our samples were from the lower respiratory tract. These were not removed from the dataset because of their low frequency and the fact that the first samples for patients are almost universally swab samples. Samples from the lower respiratory tract are generally taken from patients only after intubation, by which point viral loads have typically fallen.

PAMS status

Metadata needed to discriminate patients into sub-cohorts based on underlying diseases, outcome, or indications for diagnostic test application, including symptomatic status, were not always available. In the absence of subject-level data, we inferred PAMS status using the type of submitting test center as an indicator, classifying subjects as PAMS at the time of testing if their first-positive sample was taken from a walk-in COVID-19 test center and the subject had no later RT-PCR test done in a hospitalised context (e.g., in a ward or an intensive care unit). The correspondence between viral load and PAMS status derived herein may therefore be less accurate than in studies with subject-level symptom data. However, we make no formal claims regarding symptomatic status, and instead emphasize the fact that these PAMS subjects were healthy enough to be presenting at walk-in COVID-19 test centres, and were therefore capable to some extent, at that time, of circulating in the general community.

Bayesian analysis of age - viral load associations

We estimated associations of viral load and age with a thin-plate spline regression using the *brms* package (58, 59) in R (60). Spline coefficients were allowed to vary between groups determined by the type of the test center and clinical status (PAMS, Hospitalised, or Other), and random intercepts captured effects of test centres. To reduce the impact of outliers we used Student-t distributed error terms. The analysis additionally accounted for baseline differences between subject groups, B.1.1.7 status, gender, and for the effect of the RT-PCR system. We also estimated the association between viral load and culture probability in order to calculate the expected culture probability at different age levels. This analysis used weakly-informative priors

and was estimated using four chains with 1000 warm-up samples and 2000 post-warm-up samples. Convergence of MCMC chains was examined by checking that Potential Scale Reduction Factors (\hat{R}) values were below 1.1. All calculations of age averages and group differences are based on posterior predictions generated from estimated model parameters. Expected probabilities of positive cultures (and their differences) were calculated by applying the posterior distribution of model parameters from the culture probability model to posterior predictions from the age association model.

Combining culture probability data

To estimate the association between viral load and culture probability, we used data previously described by Wölfel (19) and Perera (20). Four other data sets could not be included because Ct values were not converted to viral loads (35, 46, 61, 62). The data from the study by van Kampen *et al.* (63) were not included because they differed (by viral load of ~ 1.0) from the data used for the current analysis, likely due to a combination of factors including many patients who were in critical or immunocompromised condition, a high proportion of samples obtained from the lower respiratory tract including late in the infectious course, and likely differences in cell culture trials. It is unsurprising that these data result in a shifted viral load / culture probability curve, and we excluded them because our focus was largely on first positive RT-PCR results from the upper respiratory tract, including from many subjects who were PAMS. The Digital Supplement shows the plot of the van Kampen data set compared to the two we used. To calculate the expected culture probability, by age (as in Fig. 2D) or by day from peak viral load (as in Fig. 4C), we combined the viral loads (Figs. 2A and 4B) with the results of the regression of culture probability shown in Fig. 2C. We used posterior predictions from the age regression model, which reflect the variation of \log_{10} viral load within age groups, to estimate culture probabilities by age. For instance, to obtain the culture probability for a specific age and group, we look up the estimated (expected) viral load for that group, add an error term, and, using the association shown in Fig. 2C, and determine the expected culture probability. We used expected time courses, i.e., the model's best guess for a time course, to estimate culture probability time courses.

B.1.1.7 isolation data

The Institute of Virology at Charité – Universitätsmedizin Berlin routinely receives SARS-CoV-2 positive samples for confirmatory testing and sequencing. For this study we used anonymized remainder samples from a large laboratory in northern Germany, that were all stored in phosphate-buffered saline (PBS) and therefore suitable for cell culture

isolation trials. Sample transport to the originating lab and later to Berlin was unrefrigerated, via road. As part of the routine testing, these samples were classified by typing RT-PCR and complete genome sequencing (64). 113 B.1.1.7 lineage samples and 110 B.1.177 lineage samples were selected, with approximately matched (pre-inoculation) SARS-CoV-2 RNA concentrations. Caco-2 (human colon carcinoma) cell cultures (65) were inoculated twice from each sample, once with undiluted material and once with a 1:10 dilution. The diluted inoculant was used to reduce the probability of culturing failure due to the possible presence of host immune factors (antibodies, cytokines, etc) that might negatively impact isolation success, and to reduce the possibility of other unrelated agents (bacteria, fungi, etc) resulting in cytopathic effect in the culture system. For cell culture isolation trials, 1.6×10^5 cells were seeded per well in a 24-well plate. Cells were inoculated with swab suspensions for one hour at 37°C, subsequently rinsed with PBS, and fed with 1 mL fresh Dulbecco's modified Eagle's minimum essential medium (DMEM; ThermoFisher Scientific) supplemented with 2% fetal bovine serum (FBS; Gibco), 100 U/mL penicillin, and 100 µg/mL streptomycin (P/S; ThermoFisher Scientific), and 2.5 µg/mL Amphotericin B (biomol) then incubated for five days before harvesting supernatant for RT-PCR testing. Positive cell culture isolation was defined by a minimum 10x higher SARS-CoV-2 RNA load in the supernatant compared to the inoculant and signs of a typical SARS-CoV-2 cytopathic effect. Culture isolation was successful for 22 B.1.1.7 and 61 B.1.177 samples. Due to uncertainty regarding sample handling before arrival at the originating diagnostic laboratory and the unrefrigerated transport, it was not possible to determine whether isolation failures were due to samples containing no infectious particles (due to sample degradation) or for other reasons. Such reasons could include systematic handling differences according to variant type or a difference in virion stability and durability regarding environmental factors such as temperature. Therefore, negative isolation outcome samples were excluded from analysis. The strong likelihood of many cases of complete sample degradation is evident from the isolation failure of many samples with high pre-inoculation viral load, with the viral load in these cases merely indicating the presence of non-infectious SARS-CoV-2 RNA (fig. S4). Given this context, we were reduced to questioning whether there might be a difference in the range of viral loads that were able to result in isolation between B.1.1.7 and non-B.1.1.7 variants. Such a difference could result from a difference in the ratio of viral RNA to infectious particles produced by the variants, or from a non-viral load difference in the variants. We examined the distribution of pre-inoculation viral loads from isolation-positive samples from both variants for a difference. No statistically significant difference was found, but

in the converse, the isolation-positive sample sizes are too low to support the assertion that the distributions do not differ.

Estimating viral load time course

Each RT-PCR test in our data set has a date, but no information regarding the suspected date of subject infection or onset of symptoms (if any). Although determining the day of peak viral load for a single person based on a series of dated RT-PCR results would not in general be feasible due to individual variation, with data from a large enough set of people, a clear and consistent model of viral load change over time can be inferred with very few assumptions.

We included a single leading and/or trailing negative RT-PCR result, if dated within seven days of the closest positive RT-PCR. To produce a model of typical viral load decline on a reasonable single-infection timescale we excluded subjects whose full time series contains positive RT-PCRs spread over a period exceeding 30 days. Such time series may be due, for example, to contamination, to later swabbing that picks up residual RNA fragments in tonsillar tissue (66), to re-infection (67–69), or may represent atypical infection courses (such as in immunocompromised or severely ill elderly patients) (70). We excluded data from subjects with an infection delimited by both an initial and a trailing negative test when there was only a single positive RT-PCR result between.

We estimated the slopes for a model of linear increase and then decline of \log_{10} viral load. To compensate for the absence of information regarding time of infection, we also estimated the number of days from infection to the first positive test for each participant, to position the observed time series relative to the day of peak viral load. The analysis was implemented in two ways. Initially, simulated annealing was used to find an optimized fit of the parameters, minimizing a least squares error function. Secondly, a Bayesian hierarchical model estimated subject-specific time courses, imputed the viral load assigned to each initial or trailing negative test, and modeled associations of age, gender, clinical status, and RT-PCR system with model parameters. We tested both methods on data subsets ranging from subjects with at least three to at least nine RT-PCR results. The two methods produced results that were in generally good agreement (table S5). The finer-grained Bayesian approach appears more sensitive than the simulated annealing and its results, for subjects with at least three RT-PCR results, are those described in the main text.

Simulated annealing approach: A simulated annealing optimization algorithm (71) was used to adjust the time series for each subject slightly earlier or later in time, by amounts drawn from a Normal distribution with mean 0.0 and standard deviation 0.1 days. The error function was the

sum of squares of distances of each viral load from a viral load decline line whose slope was also adjusted as part of the annealing process. In the error calculation, negative test results were assigned a viral load of 2.0, in accordance with our SARS-CoV-2 assay limit of detection and sample dilution (19). The initial slope of the decline line was set to -2.0 and was varied using $N(0, 0.01)$. A second, optional, increase line initialized with a slope of 2.0, adjusted using an $N(0, 0.01)$ random variable, was included in the error computation if the day of a RT-PCR test was moved earlier than day zero (the modeled day of peak viral load). The height of the intercept (i.e., the estimated peak viral load) between the increase line (if any) and the decline line was also allowed to vary randomly (starting value 10.0, varied using $N(0, 0.1)$). The full time series for each subject was initialised to a begin with the first positive result positioned at day 2 + $N(0.0, 0.5)$ post peak viral load. The random move step of the simulated annealing modified either of the two slopes or the intercept, each with probability 0.01, otherwise (with probability 0.97) one subject's time series was randomly chosen to be adjusted earlier or later in time. After the simulated annealing stage, each time series was adjusted to an improved fit (when possible), based on the optimized increase and decline lines. Linear regression lines were then fitted through the results occurring before and after the peak viral load ($x = 0$) and compared to the lines with slopes optimized by the simulated annealing alone. This final step helped to fine-tune the simulated annealing, in particular sometimes placing a time series much earlier or much later in time after it had stochastically moved initially in a direction that later (when the increase and decline line slopes had converged) proved to be sub-optimal. The slopes of the lines fitted via linear regression after this final step were in all cases very similar (generally ± 0.1) to those produced by the initial simulated annealing step. The final adjustments can be regarded as a last step in the optimization, using a steepest-descent movement operator instead of an uninformed random one. A representative optimization run for subjects with at least three RT-PCR results is shown in fig. S12.

Bayesian approach: The Bayesian analysis of viral load time course implements the same basic model, and additionally estimates associations of model parameters with covariates age, sex, B.1.1.7 status, and clinical status, estimates subject-level parameters (slope of \log_{10} load increase, peak viral load, slope of \log_{10} load decrease) as random effects, and accounts for effects of PCR system and test center types with random effects. To estimate the number of days from infection to the first test (henceforth 'shift') we constrained the possible shift values from -10 to 20 days and used a uniform prior on the support. In contrast to the other subject-level parameters, we estimated subject-level shifts

independently, i.e., without a hierarchical structure. Fig. S7 shows the placement in time of individual viral loads after shifting for subjects with RT-PCR results from at least three days. Model parameters changed gradually when subsets of subjects with an increasing minimum number of RT-PCR results, from three to nine, were examined (fig. S11 and table S5). The viral load assigned to negative test results (which may include viral loads below the level of detection) is estimated with a uniform prior on the support from $-\text{Inf}$ to 3 (see also the caption of fig. S7). Using prior predictive distributions we specified (weakly) informative priors for this analysis. This analysis was implemented in Stan (72). Full details and R and Stan code for the Bayesian analysis, as well as comparison of priors and posteriors, are given in the supplementary materials.

Checking convergence of the model parameters showed that while 99.3% of all parameters converged with an R-hat value below 1.1, some subject-level parameters of 118 subjects (among 4344 subjects with at least 3 RT-PCR results) showed R-hat values between 1.1 and 1.74. Inspection of these parameters showed that these convergence difficulties were due to observed time courses that could arguably be placed equally well at the beginning or a later stage of the infection. Figure S16 shows a set of 81 randomly-selected posterior predictions, to give an impression of time series placement, while fig. S17 shows the 49 participants with the parameters with the highest R-hat values. While the high R-hat values could be removed by using a mixture approach to model shift for these participants, in light of their low frequency we retained the simpler model to avoid additional complexity. Alternatively, constraining the shift parameter to negative numbers would also improve R-hat values for these subjects, at the cost of the additional assumption that infections are generally not detected weeks after infection.

Sensitivity analysis: In addition to examining the viral load time series of subjects with RT-PCR results on at least three days, we tested both approaches on data from subjects with results from a minimum of four to nine days. Given the degree of temporal viral load variation seen in other studies (18–20, 35, 41, 46, 63, 73, 74), and in our own data, our expectation was that a relatively high minimum number of results might be required before reliable parameter estimates with small variance would be obtained, but this proved not to be the case. The simulated annealing approach was tested with a wide range of initial slopes and intercept heights as well as seven different methods for the initial placement of time series. In general, maximum viral load and decline slopes were robust to data subset and initial time series location, though there was variation in the length of the time to peak viral load, depending on how early in time the time series were initially positioned, the initial slope of the increase line and height of the maximum viral

load, etc. This is as expected as the settings of these parameters can be used to bias the probability that a time series is initially positioned early or late in time and how difficult it is for it to subsequently move to the other side of the peak viral load at day zero. Table S5 shows parameter values for both approaches on the various data subsets.

Day of infection: We define the moment of infection as the time point at which the increasing viral load crosses zero of the \log_{10} y-axis, i.e., when just one viral particle was estimated to be present. Because the time of infection depends on the estimated peak viral load and the slope with which viral load increases, the data should optimally include multiple pre-peak viral load test results for each individual. If, as in the current data set, only a subset of subjects have test results from pre-peak viral load, a hierarchical modeling approach still allows calculating subject-level estimates. Intuitively, this approach uses data from all subjects to calculate an average slope parameter for increasing viral load. In addition, it models subject-level parameters as varying around the group level parameter. To further refine the estimation of slope parameters the model also uses the covariates age (see fig. S10), gender, and clinical status. Because negative test results could be false negatives, viral loads for these tests are imputed (with an upper bound of 3). Subject-level peak viral load and declining slope are modeled with the same approach. More generally, using a hierarchical model and shrinkage priors for covariates effects results in more accurate predictions in terms of expected squared error (75) compared to analyzing each subject in isolation, but the overall improvement introduces a slight bias toward the group mean, resulting in an underestimation of the true variability of subject-level parameters. This is especially the case if, as in the current data set, subject-level data are sparse.

Onset of symptoms: The 317 onset of symptoms dates for hospitalised patients were collected as part of the Pa-COVID-19 study, a prospective observational cohort study at Charité – Universitätsmedizin Berlin (76, 77), approved by the local ethics committee (EA2/066/20), conducted according to the Declaration of Helsinki and Good Clinical Practice principles (ICH 1996), and registered in the German and WHO international clinical trials registry (DRKS00021688).

Software

The following Python (version 3.8.2) software packages were used in the data analysis and in the production of figures: Scipy (version 1.4.1) (78), pandas (version 1.0.3) (79), statsmodels (version 0.11.1) (80), matplotlib (version 3.2.1) (81), numpy (1.18.3) (82), seaborn_sinaplot (83), simanneal (version 0.5.0) (71), and seaborn (version 0.10.1) (84). Sequence analysis used Bowtie2 (2.4.1) (85), bcftools and samtools (1.9) (86, 87), Geneious Prime (2021.0.3) (88), ivar (1.2.2)

(89), and MAFFT (4.475) (90). Analyses in R (4.0.2) (60) were conducted using the following main packages: brms (2.13.9) (58, 59), rstanarm (2.21.1) (91), rstan (2.21.2) (92), data.table (1.13.3) (93), and ggplot2 (3.3.2) (94). Bayesian analysis in R was based on Stan (2.25) (72). Parallel execution was performed with GNU Parallel (20201122 ('Biden') (95)).

Data curation and anonymization

Research clearance for the use of routine data from anonymized subjects is provided under paragraph 25 of the Berlin *Landeskrankenhausesgesetz*. All data are anonymized before processing to ensure that it is not possible to infer patient identity from any processing result. All patient information is securely combined into a token that is then replaced with a value from a strong one-way hash function prior to the distribution of data for analysis. Viral loads are calculated from RT-PCR cycle threshold values that have only one decimal place of precision.

REFERENCES AND NOTES

1. S. Lee, T. Kim, E. Lee, C. Lee, H. Kim, H. Rhee, S. Y. Park, H.-J. Son, S. Yu, J. W. Park, E. J. Choo, S. Park, M. Loeb, T. H. Kim, Clinical Course and Molecular Viral Shedding Among Asymptomatic and Symptomatic Patients With SARS-CoV-2 Infection in a Community Treatment Center in the Republic of Korea. *JAMA Intern. Med.* **180**, 1447–1452 (2020). [doi:10.1001/jamainternmed.2020.3862](https://doi.org/10.1001/jamainternmed.2020.3862) [Medline](#)
2. C. M. Szablewski, K. T. Chang, M. M. Brown, V. T. Chu, A. R. Yousaf, N. Anyalechi, P. A. Aryee, H. L. Kirking, M. Lumsden, E. Mayweather, C. J. McDaniel, R. Montieth, A. Mohammed, N. G. Schwartz, J. A. Shah, J. E. Tate, E. Dirlikov, C. Drenzek, T. M. Lanzieri, R. J. Stewart, SARS-CoV-2 Transmission and Infection Among Attendees of an Overnight Camp - Georgia, June 2020. *MMWR Morb. Mortal. Wkly. Rep.* **69**, 1023–1025 (2020). [doi:10.15585/mmwr.mm6931e1](https://doi.org/10.15585/mmwr.mm6931e1) [Medline](#)
3. Q.-X. Long, X.-J. Tang, Q.-L. Shi, Q. Li, H.-J. Deng, J. Yuan, J.-L. Hu, W. Xu, Y. Zhang, F.-J. Lv, K. Su, F. Zhang, J. Gong, B. Wu, X.-M. Liu, J.-J. Li, J.-F. Qiu, J. Chen, A.-L. Huang, Clinical and immunological assessment of asymptomatic SARS-CoV-2 infections. *Nat. Med.* **26**, 1200–1204 (2020). [doi:10.1038/s41591-020-0965-6](https://doi.org/10.1038/s41591-020-0965-6) [Medline](#)
4. Q. Bi, Y. Wu, S. Mei, C. Ye, X. Zou, Z. Zhang, X. Liu, L. Wei, S. A. Truelove, T. Zhang, W. Gao, C. Cheng, X. Tang, X. Wu, Y. Wu, B. Sun, S. Huang, Y. Sun, J. Zhang, T. Ma, J. Lessler, T. Feng, Epidemiology and transmission of COVID-19 in 391 cases and 1286 of their close contacts in Shenzhen, China: A retrospective cohort study. *Lancet Infect. Dis.* **20**, 911–919 (2020). [doi:10.1016/S1473-3099\(20\)30287-5](https://doi.org/10.1016/S1473-3099(20)30287-5) [Medline](#)
5. T. Waterfield, C. Watson, R. Moore, K. Ferris, C. Tonry, A. Watt, C. McGinn, S. Foster, J. Evans, M. D. Lyttle, S. Ahmad, S. Ladhani, M. Corr, L. McFetridge, H. Mitchell, K. Brown, G. Amirhalingam, J.-A. Maney, S. Christie, Seroprevalence of SARS-CoV-2 antibodies in children: A prospective multicentre cohort study. *Arch. Dis. Child.* [10.1136/archdischild-2020-320558](https://doi.org/10.1136/archdischild-2020-320558) (2020). [doi:10.1136/archdischild-2020-320558](https://doi.org/10.1136/archdischild-2020-320558) [Medline](#)
6. D. C. Adam, P. Wu, J. Y. Wong, E. H. Y. Lau, T. K. Tsang, S. Cauchemez, G. M. Leung, B. J. Cowling, Clustering and superspreading potential of SARS-CoV-2 infections in Hong Kong. *Nat. Med.* **26**, 1714–1719 (2020). [Medline](#)
7. M. Hippich, L. Holthaus, R. Assfalg, J. M. Zapardiel Gonzalo, H. Kapfelsperger, M. Heigermoser, F. Haupt, D. A. Ewald, T. C. Welzhofer, B. A. Marcus, S. Heck, A. Koelln, J. Stock, F. Voss, M. Secchi, L. Piemonti, K. de la Rosa, U. Protzer, M.

- Boehmer, P. Achenbach, V. Lampasona, E. Bonifacio, A.-G. Ziegler, A public health antibody screening indicates a six-fold higher SARS-CoV-2 exposure rate than reported cases in children. *Med* **2**, 149–163.e4 (2020). [doi:10.1016/j.medj.2020.10.003](https://doi.org/10.1016/j.medj.2020.10.003)
8. E. Lavezzo, E. Franchin, C. Ciavarella, G. Cuomo-Dannenburg, L. Barzon, C. Del Vecchio, L. Rossi, R. Manganeli, A. Loregian, N. Navarin, D. Abate, M. Sciro, S. Merigliano, E. De Canale, M. C. Vanuzzo, V. Besutti, F. Saluzzo, F. Onelia, M. Pacenti, S. G. Parisi, G. Carretta, D. Donato, L. Flor, S. Cocchio, G. Masi, A. Sperduti, L. Cattarino, R. Salvador, M. Nicoletti, F. Caldart, G. Castelli, E. Nieldu, B. Labella, L. Fava, M. Drigo, K. A. M. Gaythorpe, A. R. Brazzale, S. Toppo, M. Trevisan, V. Baldo, C. A. Donnelly, N. M. Ferguson, I. Dorigatti, A. Crisanti, Imperial College COVID-19 Response Team, Imperial College COVID-19 Response Team, Suppression of a SARS-CoV-2 outbreak in the Italian municipality of Vo'. *Nature* **584**, 425–429 (2020). [doi:10.1038/s41586-020-2488-1](https://doi.org/10.1038/s41586-020-2488-1) [Medline](#)
9. M. Marks, P. Millat-Martinez, D. Ouchi, C. H. Roberts, A. Alemany, M. Corbacho-Monné, M. Ubals, A. Tobias, C. Tebé, E. Ballana, Q. Bassat, B. Baro, M. Vall-Mayans, C. G-Beiras, N. Prat, J. Ara, B. Clotet, O. Mitjà, Transmission of COVID-19 in 282 clusters in Catalonia, Spain: A cohort study. *Lancet Infect. Dis.* **21**, 629–636 (2021). [doi:10.1016/S1473-3099\(20\)30985-3](https://doi.org/10.1016/S1473-3099(20)30985-3) [Medline](#)
10. L. L. H. Lau, B. J. Cowling, V. J. Fang, K.-H. Chan, E. H. Y. Lau, M. Lipsitch, C. K. Y. Cheng, P. M. Houck, T. M. Uyeki, J. S. M. Peiris, G. M. Leung, Viral shedding and clinical illness in naturally acquired influenza virus infections. *J. Infect. Dis.* **201**, 1509–1516 (2010). [doi:10.1086/652241](https://doi.org/10.1086/652241) [Medline](#)
11. T. K. Tsang, V. J. Fang, K.-H. Chan, D. K. M. Ip, G. M. Leung, J. S. M. Peiris, B. J. Cowling, S. Cauchemez, Individual Correlates of Infectivity of Influenza A Virus Infections in Households. *PLoS ONE* **11**, e0154418 (2016). [doi:10.1371/journal.pone.0154418](https://doi.org/10.1371/journal.pone.0154418) [Medline](#)
12. E. A. Meyerowitz, A. Richterman, I. I. Bogoch, N. Low, M. Cevik, Towards an accurate and systematic characterisation of persistently asymptomatic infection with SARS-CoV-2. *Lancet Infect. Dis.* **S1473-3099(20)30837-9** (2020). [doi:10.1016/S1473-3099\(20\)30837-9](https://doi.org/10.1016/S1473-3099(20)30837-9) [Medline](#)
13. A. Fontanet, L. Tondeur, R. Grant, S. Temmam, Y. Madec, T. Bigot, L. Grzelak, I. Cailleau, C. Besombes, M.-N. Ungeheuer, C. Renaudat, B. L. Perlaza, L. Arowas, N. Jolly, S. F. Pellerin, L. Kuhmel, I. Staropoli, C. Huon, K.-Y. Chen, B. Crescenzo-Chaigne, S. Munier, P. Charneau, C. Demeret, T. Bruel, M. Eloit, O. Schwartz, B. Hoen, SARS-CoV-2 infection in schools in a northern French city: A retrospective serological cohort study in an area of high transmission, France, January to April 2020. *Euro Surveill.* **26**, 2001695 (2021). [doi:10.2807/1560-7917.ES.2021.26.15.2001695](https://doi.org/10.2807/1560-7917.ES.2021.26.15.2001695)
14. C. Stein-Zamir, N. Abramson, H. Shoob, E. Libal, M. Bitan, T. Cardash, R. Cayam, I. Miskin, A large COVID-19 outbreak in a high school 10 days after schools' reopening, Israel, May 2020. *Euro Surveill.* **25**, (2020). [doi:10.2807/1560-7917.ES.2020.25.29.2001352](https://doi.org/10.2807/1560-7917.ES.2020.25.29.2001352) [Medline](#)
15. I. W. Pray, S. N. Gibbons-Burgener, A. Z. Rosenberg, D. Cole, S. Borenstein, A. Bateman, E. Pevzner, R. P. Westergaard, COVID-19 Outbreak at an Overnight Summer School Retreat - Wisconsin, July-August 2020. *MMWR Morb. Mortal. Wkly. Rep.* **69**, 1600–1604 (2020). [doi:10.15585/mmwr.mm6943a4](https://doi.org/10.15585/mmwr.mm6943a4) [Medline](#)
16. J. P. Torres, C. Piñera, V. De La Maza, A. J. Lagomarcino, D. Simian, B. Torres, C. Urquidi, M. T. Valenzuela, M. O'Ryan, SARS-CoV-2 antibody prevalence in blood in a large school community subject to a Covid-19 outbreak: A cross-sectional study. *Clin. Infect. Dis.* **ciaa955** (2020). [doi:10.1093/cid/ciaa955](https://doi.org/10.1093/cid/ciaa955) [Medline](#)
17. M. H. Ebell, C. Chupp, M. Bentivegna, A high proportion of SARS-CoV-2-infected university students are asymptomatic. *J. Fam. Pract.* **69**, 428–429 (2020). [Medline](#)
18. S. M. Kissler *et al.*, Viral dynamics of SARS-CoV-2 infection and the predictive value of repeat testing. *medRxiv* **20217042** [preprint]. 23 October 2020.
19. R. Wölfel, V. M. Corman, W. Guggemos, M. Seilmaier, S. Zange, M. A. Müller, D. Niemeyer, T. C. Jones, P. Vollmar, C. Rothe, M. Hoelscher, T. Bleicker, S. Brünink, J. Schneider, R. Ehmann, K. Zwirgmaier, C. Drosten, C. Wendtner, Virological assessment of hospitalized patients with COVID-2019. *Nature* **581**, 465–469 (2020). [doi:10.1038/s41586-020-2196-x](https://doi.org/10.1038/s41586-020-2196-x) [Medline](#)
20. R. A. P. M. Perera, E. Tso, O. T. Y. Tsang, D. N. C. Tsang, K. Fung, Y. W. Y. Leung, A. W. H. Chin, D. K. W. Chu, S. M. S. Cheng, L. L. M. Poon, V. W. M. Chuang, M. Peiris, SARS-CoV-2 Virus Culture and Subgenomic RNA for Respiratory Specimens from Patients with Mild Coronavirus Disease. *Emerg. Infect. Dis.* **26**, 2701–2704 (2020). [doi:10.3201/eid2611.203219](https://doi.org/10.3201/eid2611.203219) [Medline](#)
21. A. Endo, S. Abbott, A. J. Kucharski, S. Funk, Centre for the Mathematical Modelling of Infectious Diseases COVID-19 Working Group, Estimating the overdispersion in COVID-19 transmission using outbreak sizes outside China. *Wellcome Open Res.* **5**, 67 (2020). [doi:10.12688/wellcomeopenres.15842.3](https://doi.org/10.12688/wellcomeopenres.15842.3) [Medline](#)
22. K. Sun, W. Wang, L. Gao, Y. Wang, K. Luo, L. Ren, Z. Zhan, X. Chen, S. Zhao, Y. Huang, Q. Sun, Z. Liu, M. Litvinova, A. Vespignani, M. Ajelli, C. Viboud, H. Yu, Transmission heterogeneities, kinetics, and controllability of SARS-CoV-2. *Science* **371**, eabe2424 (2021). [Medline](#)
23. N. J. Lennon, R. P. Bhattacharyya, M. J. Mina, H. L. Rehm, D. T. Hung, S. Smole, A. Woolley, E. S. Lander, S. B. Gabriel, Comparison of viral levels in individuals with or without symptoms at time of COVID-19 testing among 32,480 residents and staff of nursing homes and assisted living facilities in Massachusetts. *Open Forum Infect. Dis.* **7** (suppl. 1), 848–849 (2020). [doi:10.1093/ofid/ofaa515.1908](https://doi.org/10.1093/ofid/ofaa515.1908)
24. R. Laxminarayan, B. Wahl, S. R. Dudala, K. Gopal, C. Mohan B, S. Neelima, K. S. Jawahar Reddy, J. Radhakrishnan, J. A. Lewnard, Epidemiology and transmission dynamics of COVID-19 in two Indian states. *Science* **370**, 691–697 (2020). [doi:10.1126/science.abd7672](https://doi.org/10.1126/science.abd7672) [Medline](#)
25. T. Suess, C. Remschmidt, S. B. Schink, B. Schweiger, A. Heider, J. Milde, A. Nitsche, K. Schroeder, J. Doellinger, C. Braun, W. Haas, G. Krause, U. Buchholz, Comparison of shedding characteristics of seasonal influenza virus (sub)types and influenza A(H1N1)pdm09; Germany, 2007–2011. *PLoS ONE* **7**, e51653 (2012). [doi:10.1371/journal.pone.0051653](https://doi.org/10.1371/journal.pone.0051653) [Medline](#)
26. M. Loeb, P. K. Singh, J. Fox, M. L. Russell, K. Pabbaraju, D. Zarra, S. Wong, B. Neupane, P. Singh, R. Webby, K. Fonseca, Longitudinal study of influenza molecular viral shedding in Hutterite communities. *J. Infect. Dis.* **206**, 1078–1084 (2012). [doi:10.1093/infdis/jis450](https://doi.org/10.1093/infdis/jis450) [Medline](#)
27. B. J. Cowling, K. H. Chan, V. J. Fang, L. L. H. Lau, H. C. So, R. O. P. Fung, E. S. K. Ma, A. S. K. Kwong, C.-W. Chan, W. W. S. Tsui, H.-Y. Ngai, D. W. S. Chu, P. W. Y. Lee, M.-C. Chiu, G. M. Leung, J. S. M. Peiris, Comparative epidemiology of pandemic and seasonal influenza A in households. *N. Engl. J. Med.* **362**, 2175–2184 (2010). [doi:10.1056/NEJMoa0911530](https://doi.org/10.1056/NEJMoa0911530) [Medline](#)
28. D. K. M. Ip, L. L. H. Lau, N. H. L. Leung, V. J. Fang, K.-H. Chan, D. K. W. Chu, G. M. Leung, J. S. M. Peiris, T. M. Uyeki, B. J. Cowling, Viral Shedding and Transmission Potential of Asymptomatic and Paucisymptomatic Influenza Virus Infections in the Community. *Clin. Infect. Dis.* **64**, 736–742 (2017). [Medline](#)
29. N. H. L. Leung, C. Xu, D. K. M. Ip, B. J. Cowling, The Fraction of Influenza Virus Infections That Are Asymptomatic: A Systematic Review and Meta-analysis. *Epidemiology* **26**, 862–872 (2015). [doi:10.1097/EDE.0000000000000340](https://doi.org/10.1097/EDE.0000000000000340) [Medline](#)
30. L. P. Moreira, A. S. A. Watanabe, C. N. Camargo, T. B. Melchior, C. Granato, N. Bellei, Respiratory syncytial virus evaluation among asymptomatic and symptomatic subjects in a university hospital in Sao Paulo, Brazil, in the period of 2009–2013. *Influenza Other Respir. Viruses* **12**, 326–330 (2018). [doi:10.1111/irv.12518](https://doi.org/10.1111/irv.12518) [Medline](#)
31. D. Jacot, G. Greub, K. Jatou, O. Oputa, Viral load of SARS-CoV-2 across patients and compared to other respiratory viruses. *Microbes Infect.* **22**, 617–621 (2020). [doi:10.1016/j.micinf.2020.08.004](https://doi.org/10.1016/j.micinf.2020.08.004) [Medline](#)
32. T. Heald-Sargent, W. J. Muller, X. Zheng, J. Rippe, A. B. Patel, L. K. Kocielek, Age-Related Differences in Nasopharyngeal Severe Acute Respiratory Syndrome Coronavirus 2 (SARS-CoV-2) Levels in Patients With Mild to Moderate Coronavirus Disease 2019 (COVID-19). *JAMA Pediatr.* **174**, 902–903 (2020). [doi:10.1001/jamapediatrics.2020.3651](https://doi.org/10.1001/jamapediatrics.2020.3651) [Medline](#)
33. L. M. Yonker, A. M. Neilan, Y. Bartsch, A. B. Patel, J. Regan, P. Arya, E. Gootkind, G. Park, M. Hardcastle, A. St. John, L. Appleman, M. L. Chiu, A. Fialkowski, D. De

- la Flor, R. Lima, E. A. Bordt, L. J. Yockey, P. D'Avino, S. Fischinger, J. E. Shui, P. H. Lerou, J. V. Bonventre, X. G. Yu, E. T. Ryan, I. V. Bassett, D. Irimia, A. G. Edlow, G. Alter, J. Z. Li, A. Fasano, Pediatric SARS-CoV-2: Clinical Presentation, Infectivity, and Immune Responses. *J. Pediatr.* **227**, 45–52.e5 (2020). [doi:10.1016/j.jpeds.2020.08.037](https://doi.org/10.1016/j.jpeds.2020.08.037) [Medline](#)
34. S. Baggio, A. G. L'Huillier, S. Yerly, M. Bellon, N. Wagner, M. Rohr, A. Huttner, G. Blanchard-Rohner, N. Loevy, L. Kaiser, F. Jacquerioz, I. Eckerle, SARS-CoV-2 viral load in the upper respiratory tract of children and adults with early acute COVID-19. *Clin. Infect. Dis.* ciaa1157 (2020). [doi:10.1093/cid/ciaa1157](https://doi.org/10.1093/cid/ciaa1157) [Medline](#)
35. A. Singanayagam, M. Patel, A. Charlett, J. Lopez Bernal, V. Saliba, J. Ellis, S. Ladhani, M. Zambon, R. Gopal, Duration of infectiousness and correlation with RT-PCR cycle threshold values in cases of COVID-19, England, January to May 2020. *Euro Surveill.* **25**, (2020). [doi:10.2807/1560-7917.ES.2020.25.32.2001483](https://doi.org/10.2807/1560-7917.ES.2020.25.32.2001483) [Medline](#)
36. V. M. Corman, V. C. Haage, T. Bleicker, M. L. Schmidt, B. Mühlemann, M. Zuchowski, W. K. Jo, P. Tscheak, E. Möncke-Buchner, M. A. Müller, A. Krumbholz, J. F. Drexler, C. Drosten, Comparison of seven commercial SARS-CoV-2 rapid point-of-care antigen tests: a single-centre laboratory evaluation study. *Lancet Microbe* 10.1016/S2666-5247(21)00056-2 (2021). [doi:10.1016/S2666-5247\(21\)00056-2](https://doi.org/10.1016/S2666-5247(21)00056-2)
37. M. S. Han, E. H. Choi, S. H. Chang, B.-L. Jin, E. J. Lee, B. N. Kim, M. K. Kim, K. Doo, J.-H. Seo, Y.-J. Kim, Y. J. Kim, J. Y. Park, S. B. Suh, H. Lee, E. Y. Cho, D. H. Kim, J. M. Kim, H. Y. Kim, S. E. Park, J. K. Lee, D. S. Jo, S.-M. Cho, J. H. Choi, K. J. Jo, Y. J. Choe, K. H. Kim, J.-H. Kim, Clinical Characteristics and Viral RNA Detection in Children With Coronavirus Disease, 2019 in the Republic of Korea. *JAMA Pediatr.* **175**, 73–80 (2021). [doi:10.1001/jamapediatrics.2020.3988](https://doi.org/10.1001/jamapediatrics.2020.3988) [Medline](#)
38. C. A. Pierce, S. Sy, B. Galen, D. Y. Goldstein, E. Orner, M. J. Keller, K. C. Herold, B. C. Herold, Natural mucosal barriers and COVID-19 in children. *JCI Insight* **6**, e148694 (2021). [doi:10.1172/jci.insight.148694](https://doi.org/10.1172/jci.insight.148694) [Medline](#)
39. Q. Li, X. Guan, P. Wu, X. Wang, L. Zhou, Y. Tong, R. Ren, K. S. M. Leung, E. H. Y. Lau, J. Y. Wong, X. Xing, N. Xiang, Y. Wu, C. Li, Q. Chen, D. Li, T. Liu, J. Zhao, M. Liu, W. Tu, C. Chen, L. Jin, R. Yang, Q. Wang, S. Zhou, R. Wang, H. Liu, Y. Luo, Y. Liu, G. Shao, H. Li, Z. Tao, Y. Yang, Z. Deng, B. Liu, Z. Ma, Y. Zhang, G. Shi, T. T. Y. Lam, J. T. Wu, G. F. Gao, B. J. Cowling, B. Yang, G. M. Leung, Z. Feng, Early Transmission Dynamics in Wuhan, China, of Novel Coronavirus-Infected Pneumonia. *N. Engl. J. Med.* **382**, 1199–1207 (2020). [doi:10.1056/NEJMoa2001316](https://doi.org/10.1056/NEJMoa2001316) [Medline](#)
40. L. Ferretti, A. Ledda, C. Wymant, L. Zhao, V. Ledda, L. Abeler-Dorner, M. Kendall, A. Nurtay, H.-Y. Cheng, T.-C. Ng, H.-H. Lin, R. Hinch, J. Masel, A. M. Kilpatrick, C. Fraser, The timing of COVID-19 transmission. medRxiv [20188516](https://doi.org/10.1101/2020.08.15.20188516) [preprint]. 7 September 2020.
41. X. He, E. H. Y. Lau, P. Wu, X. Deng, J. Wang, X. Hao, Y. C. Lau, J. Y. Wong, Y. Guan, X. Tan, X. Mo, Y. Chen, B. Liao, W. Chen, F. Hu, Q. Zhang, M. Zhong, Y. Wu, L. Zhao, F. Zhang, B. J. Cowling, F. Li, G. M. Leung, Temporal dynamics in viral shedding and transmissibility of COVID-19. *Nat. Med.* **26**, 672–675 (2020). [doi:10.1038/s41591-020-0869-5](https://doi.org/10.1038/s41591-020-0869-5) [Medline](#)
42. C. McAloon, Á. Collins, K. Hunt, A. Barber, A. W. Byrne, F. Butler, M. Casey, J. Griffin, E. Lane, D. McEvoy, P. Wall, M. Green, L. O'Grady, S. J. More, Incubation period of COVID-19: A rapid systematic review and meta-analysis of observational research. *BMJ Open* **10**, e039652 (2020). [doi:10.1136/bmjopen-2020-039652](https://doi.org/10.1136/bmjopen-2020-039652) [Medline](#)
43. P. Banka, C. Comiskey, The incubation period of COVID-19: A scoping review and meta-analysis to aid modelling and planning. medRxiv [2021.06.14.21261443](https://doi.org/10.1101/2021.06.14.21261443) [preprint]. 3 November 2020.
44. B. Rai, A. Shukla, L. K. Dwivedi, Incubation period for COVID-19: A systematic review and meta-analysis. *J. Public Health* 10.1007/s10389-021-01478-1 (2021). [doi:10.1007/s10389-021-01478-1](https://doi.org/10.1007/s10389-021-01478-1) [Medline](#)
45. J. Bullard, K. Dust, D. Funk, J. E. Strong, D. Alexander, L. Garnett, C. Boodman, A. Bello, A. Hedley, Z. Schiffman, K. Doan, N. Bastien, Y. Li, P. G. Van Caesele, G. Poliquin, Predicting infectious SARS-CoV-2 from diagnostic samples. *Clin. Infect. Dis.* **71**, 2663–2666 (2020). [doi:10.1093/cid/ciaa638](https://doi.org/10.1093/cid/ciaa638)
46. M. M. Arons, K. M. Hatfield, S. C. Reddy, A. Kimball, A. James, J. R. Jacobs, J. Taylor, K. Spicer, A. C. Bardossy, L. P. Oakley, S. Tanwar, J. W. Dyal, J. Harney, Z. Chisty, J. M. Bell, M. Methner, P. Paul, C. M. Carlson, H. P. McLaughlin, N. Thornburg, S. Tong, A. Tamin, Y. Tao, A. Uehara, J. Harcourt, S. Clark, C. Brostrom-Smith, L. C. Page, M. Kay, J. Lewis, P. Montgomery, N. D. Stone, T. A. Clark, M. A. Honein, J. S. Duchin, J. A. Jernigan, Public Health–Seattle and King County and CDC COVID-19 Investigation Team, Presymptomatic SARS-CoV-2 Infections and Transmission in a Skilled Nursing Facility. *N. Engl. J. Med.* **382**, 2081–2090 (2020). [doi:10.1056/NEJMoa2008457](https://doi.org/10.1056/NEJMoa2008457) [Medline](#)
47. K. R. W. Emary, T. Golubchik, Efficacy of ChAdOx1 nCoV-19 (AZD1222) vaccine against SARS-CoV-2 VOC 202012/01 (B.1.1.7). SSRN [preprint]. 4 February 2021; <https://ssrn.com/abstract=3779160>.
48. R. Challen, E. Brooks-Pollock, J. M. Read, L. Dyson, K. Tsaneva-Atanasova, L. Danon, Risk of mortality in patients infected with SARS-CoV-2 variant of concern 202012/1: Matched cohort study. *BMJ* **372**, n579 (2021). [doi:10.1136/bmj.n579](https://doi.org/10.1136/bmj.n579) [Medline](#)
49. M. D. Parker *et al.*, Altered subgenomic RNA expression in SARS-CoV-2 B.1.1.7 infections. bioRxiv [433156](https://doi.org/10.1101/2021.03.04.433156) [preprint]. 4 March 2021.
50. M. Kidd, A. Richter, A. Best, N. Cumley, J. Mirza, B. Percival, M. Mayhew, O. Megram, F. Ashford, T. White, E. Moles-Garcia, L. Crawford, A. Bosworth, S. F. Atabani, T. Plant, A. McNally, S-variant SARS-CoV-2 lineage B.1.1.7 is associated with significantly higher viral loads in samples tested by TaqPath Polymerase Chain Reaction. *J. Infect. Dis.* [jiab082](https://doi.org/10.1093/infdis/jiab082) (2021). [doi:10.1093/infdis/jiab082](https://doi.org/10.1093/infdis/jiab082) [Medline](#)
51. T. Golubchik, K. A. Lythgoe, M. Hall, L. Ferretti, H. R. Fryer, G. MacIntyre-Cockett, M. de Cesare, A. Trebes, P. Piazza, D. Buck, J. A. Todd, C. Fraser, D. Bonsall, COVID-19 Genomics UK (COG-UK) Consortium, Early analysis of a potential link between viral load and the N501Y mutation in the SARS-CoV-2 spike protein. medRxiv [20249080](https://doi.org/10.1101/2021.01.15.20249080) [preprint]. 15 January 2021.
52. S. Kissler *et al.*, “Densely sampled viral trajectories suggest longer duration of acute infection with B.1.1.7 variant relative to non-B.1.1.7 SARS-CoV-2” (Harvard T. H. Chan School of Public Health, 2021); <https://dash.harvard.edu/handle/1/37366884>.
53. Public Health England, “Investigation of novel SARS-CoV-2 Variant of Concern 202012/01: Technical briefing 5” (2021).
54. K. Leung, M. H. Shum, G. M. Leung, T. T. Lam, J. T. Wu, Early transmissibility assessment of the N501Y mutant strains of SARS-CoV-2 in the United Kingdom, October to November 2020. *Euro Surveill.* **26**, (2021). [doi:10.2807/1560-7917.ES.2020.26.1.2002106](https://doi.org/10.2807/1560-7917.ES.2020.26.1.2002106) [Medline](#)
55. N. G. Davies, S. Abbott, R. C. Barnard, C. I. Jarvis, A. J. Kucharski, J. D. Munday, C. A. B. Pearson, T. W. Russell, D. C. Tully, A. D. Washburne, T. Wenseleers, A. Gimma, W. Waites, K. L. M. Wong, K. van Zandvoort, J. D. Silverman, K. Diaz-Ordaz, R. Keogh, R. M. Eggo, S. Funk, M. Jit, K. E. Atkins, W. J. Edmunds, CMMID COVID-19 Working Group, COVID-19 Genomics UK (COG-UK) Consortium, Estimated transmissibility and impact of SARS-CoV-2 lineage B.1.1.7 in England. *Science* **372**, eabg3055 (2021). [doi:10.1126/science.abg3055](https://doi.org/10.1126/science.abg3055) [Medline](#)
56. R. Li, S. Pei, B. Chen, Y. Song, T. Zhang, W. Yang, J. Shaman, Substantial undocumented infection facilitates the rapid dissemination of novel coronavirus (SARS-CoV-2). *Science* **368**, 489–493 (2020). [doi:10.1126/science.abb3221](https://doi.org/10.1126/science.abb3221) [Medline](#)
57. Public Health England, “Investigation of novel SARS-CoV-2 Variant of Concern 202012/01: Technical briefing 1” (2020).
58. P.-C. Bürkner, brms: An R Package for Bayesian Multilevel Models Using Stan. *J. Stat. Softw.* **80**, (2017). [doi:10.18637/jss.v080.i01](https://doi.org/10.18637/jss.v080.i01)
59. P.-C. Bürkner, Advanced Bayesian Multilevel Modeling with the R Package brms. *R J.* **10**, 395 (2018). [doi:10.32614/RJ-2018-017](https://doi.org/10.32614/RJ-2018-017)
60. R Core Team, *R: A Language and Environment for Statistical Computing* (R Foundation for Statistical Computing, 2020); www.R-project.org/.
61. K. Basile, K. McPhie, I. Carter, S. Alderson, H. Rahman, L. Donovan, S. Kumar, T. Tran, D. Ko, T. Sivaruban, C. Ngo, C. Toi, M. V. O'Sullivan, V. Sintchenko, S. C.-A. Chen, S. Maddocks, D. E. Dwyer, J. Kok, Cell-based culture of SARS-CoV-2 informs infectivity and safe de-isolation assessments during COVID-19. *Clin.*

- Infect. Dis.* ciaa1579 (2020). [doi:10.1093/cid/ciaa1579](https://doi.org/10.1093/cid/ciaa1579) [Medline](#)
62. B. La Scola, M. Le Bideau, J. Andreani, V. T. Hoang, C. Grimaldier, P. Colson, P. Gautret, D. Raoult, Viral RNA load as determined by cell culture as a management tool for discharge of SARS-CoV-2 patients from infectious disease wards. *Eur. J. Clin. Microbiol. Infect. Dis.* **39**, 1059–1061 (2020). [doi:10.1007/s10096-020-03913-9](https://doi.org/10.1007/s10096-020-03913-9) [Medline](#)
63. J. J. A. van Kampen, D. A. M. C. van de Vijver, P. L. A. Fraaij, B. L. Haagmans, M. M. Lamers, N. Okba, J. P. C. van den Akker, H. Endeman, D. A. M. P. J. Gommers, J. J. Cornelissen, R. A. S. Hoek, M. M. van der Eerden, D. A. Hesselink, H. J. Metselaar, A. Verbon, J. E. M. de Steenwinkel, G. I. Aron, E. C. M. van Gorp, S. van Boheemen, J. C. Voermans, C. A. B. Boucher, R. Molenkamp, M. P. G. Koopmans, C. Geurtsvankessel, A. A. van der Eijk, Duration and key determinants of infectious virus shedding in hospitalized patients with coronavirus disease-2019 (COVID-19). *Nat. Commun.* **12**, 267 (2021). [doi:10.1038/s41467-020-20568-4](https://doi.org/10.1038/s41467-020-20568-4) [Medline](#)
64. M. Widera, B. Mühlemann, V. M. Corman, T. Toptan, J. Beheim-Schwarzbach, N. Kohmer, J. Schneider, A. Berger, T. Veith, C. Pallas, T. Bleicker, U. Goetsch, J. Tesch, R. Gottschalk, T. C. Jones, S. Ciesek, C. Drosten, Surveillance of SARS-CoV-2 in Frankfurt am Main from October to December 2020 Reveals High Viral Diversity Including Spike Mutation N501Y in B.1.1.70 and B.1.1.7. *Microorganisms* **9**, 748 (2021). [doi:10.3390/microorganisms9040748](https://doi.org/10.3390/microorganisms9040748) [Medline](#)
65. T. Toptan, L. Eckermann, A. E. Pfeiffer, S. Hoehl, S. Ciesek, C. Drosten, V. M. Corman, Evaluation of a SARS-CoV-2 rapid antigen test: Potential to help reduce community spread? *J. Clin. Virol.* **135**, 104713 (2021). [doi:10.1016/j.jcv.2020.104713](https://doi.org/10.1016/j.jcv.2020.104713) [Medline](#)
66. S. Herberhold, A.-M. Eis-Hübinger, M. Panning, Frequent detection of respiratory viruses by real-time PCR in adenoid samples from asymptomatic children. *J. Clin. Microbiol.* **47**, 2682–2683 (2009). [doi:10.1128/JCM.00899-09](https://doi.org/10.1128/JCM.00899-09) [Medline](#)
67. F. M. Liotti, G. Menchinelli, S. Marchetti, B. Posteraro, F. Landi, M. Sanguinetti, P. Cattani, Assessment of SARS-CoV-2 RNA Test Results Among Patients Who Recovered From COVID-19 With Prior Negative Results. *JAMA Intern. Med.* **181**, 702–704 (2021). [doi:10.1001/jamainternmed.2020.7570](https://doi.org/10.1001/jamainternmed.2020.7570) [Medline](#)
68. R. L. Tillett, J. R. Sevinsky, P. D. Hartley, H. Kerwin, N. Crawford, A. Gorzalski, C. Laverdure, S. C. Verma, C. C. Rossetto, D. Jackson, M. J. Farrell, S. Van Hooser, M. Pandori, Genomic evidence for reinfection with SARS-CoV-2: A case study. *Lancet Infect. Dis.* **21**, 52–58 (2021). [doi:10.1016/S1473-3099\(20\)30764-7](https://doi.org/10.1016/S1473-3099(20)30764-7) [Medline](#)
69. K. K.-W. To, I. F.-N. Hung, J. D. Ip, A. W.-H. Chu, W.-M. Chan, A. R. Tam, C. H.-Y. Fong, S. Yuan, H.-W. Tsoi, A. C.-K. Ng, L. L.-Y. Lee, P. Wan, E. Y.-K. Tso, W.-K. To, D. N.-C. Tsang, K.-H. Chan, J.-D. Huang, K.-H. Kok, V. C.-C. Cheng, K.-Y. Yuen, Coronavirus Disease 2019 (COVID-19) Re-infection by a Phylogenetically Distinct Severe Acute Respiratory Syndrome Coronavirus 2 Strain Confirmed by Whole Genome Sequencing. *Clin. Infect. Dis.* **9**, 1664 (2020).
70. P. Simmonds, S. Williams, H. Harvala, Understanding the outcomes of COVID-19 – does the current model of an acute respiratory infection really fit? *J. Gen. Virol.* **102**, 10.1099/jgv.0.001545 (2020). [doi:10.1099/jgv.0.001545](https://doi.org/10.1099/jgv.0.001545) [Medline](#)
71. M. Perry, simanneal: A Python Module for Simulated Annealing Optimization; <https://github.com/perrygeo/simanneal>.
72. Stan Development Team, Stan Modeling Language Users Guide and Reference Manual (version 2.25); <https://mc-stan.org>.
73. Y. Liu, L.-M. Yan, L. Wan, T.-X. Xiang, A. Le, J.-M. Liu, M. Peiris, L. L. M. Poon, W. Zhang, Viral dynamics in mild and severe cases of COVID-19. *Lancet Infect. Dis.* **20**, 656–657 (2020). [doi:10.1016/S1473-3099\(20\)30232-2](https://doi.org/10.1016/S1473-3099(20)30232-2) [Medline](#)
74. K. K.-W. To, O. T.-Y. Tsang, W.-S. Leung, A. R. Tam, T.-C. Wu, D. C. Lung, C. C.-Y. Yip, J.-P. Cai, J. M.-C. Chan, T. S.-H. Chik, D. P.-L. Lau, C. Y.-C. Choi, L.-L. Chen, W.-M. Chan, K.-H. Chan, J. D. Ip, A. C.-K. Ng, R. W.-S. Poon, C.-T. Luo, V. C.-C. Cheng, J. F.-W. Chan, I. F.-N. Hung, Z. Chen, H. Chen, K.-Y. Yuen, Temporal profiles of viral load in posterior oropharyngeal saliva samples and serum antibody responses during infection by SARS-CoV-2: An observational cohort study. *Lancet Infect. Dis.* **20**, 565–574 (2020). [doi:10.1016/S1473-3099\(20\)30196-1](https://doi.org/10.1016/S1473-3099(20)30196-1) [Medline](#)
75. S. Greenland, Principles of multilevel modelling. *Int. J. Epidemiol.* **29**, 158–167 (2000). [doi:10.1093/ije/29.1.158](https://doi.org/10.1093/ije/29.1.158) [Medline](#)
76. F. Kurth, M. Roenefarth, C. Thibeault, V. M. Corman, H. Müller-Redetzky, M. Mittermaier, C. Ruwwe-Glösenkamp, K. M. Heim, A. Krannich, S. Zvorc, S. Schmidt, L. Kretzler, C. Dang-Heine, M. Rose, M. Hummel, A. Hocke, R. H. Hübner, B. Opitz, M. A. Mall, J. Röhmel, U. Landmesser, B. Pieske, S. Knauss, M. Endres, J. Spranger, F. P. Mockenhaupt, F. Tacke, S. Treskatsch, S. Angermair, B. Siegmund, C. Spies, S. Weber-Carstens, K.-U. Eckardt, D. Schürmann, A. Uhrig, M. S. Stegemann, T. Zoller, C. Drosten, N. Suttrop, M. Witzenrath, S. Hippenstiel, C. von Kalle, L. E. Sander, Studying the pathophysiology of coronavirus disease 2019: A protocol for the Berlin prospective COVID-19 patient cohort (Pa-COVID-19). *Infection* **48**, 619–626 (2020). [doi:10.1007/s15010-020-01464-x](https://doi.org/10.1007/s15010-020-01464-x) [Medline](#)
77. C. Thibeault, B. Mühlemann, E. T. Helbig, M. Mittermaier, T. Lingscheid, P. Tober-Lau, L. A. Meyer-Arndt, L. Meiners, P. Stubbemann, S. S. Haenel, L. Bosquillon de Jarcy, L. Lippert, M. Pfeiffer, M. S. Stegemann, R. Roehle, J. Wiebach, S. Hippenstiel, T. Zoller, H. Müller-Redetzky, A. Uhrig, F. Balzer, C. von Kalle, N. Suttrop, T. C. Jones, C. Drosten, M. Witzenrath, L. E. Sander, V. M. Corman, F. Kurth, Pa-COVID Study Group, Clinical and virological characteristics of hospitalised COVID-19 patients in a German tertiary care centre during the first wave of the SARS-CoV-2 pandemic: A prospective observational study. *Infection* **10.1007/s15010-021-01594-w** (2021). [doi:10.1007/s15010-021-01594-w](https://doi.org/10.1007/s15010-021-01594-w) [Medline](#)
78. P. Virtanen, R. Gommers, T. E. Oliphant, M. Haberland, T. Reddy, D. Cournapeau, E. Burovski, P. Peterson, W. Weckesser, J. Bright, S. J. van der Walt, M. Brett, J. Wilson, K. J. Millman, N. Mayorov, A. R. J. Nelson, E. Jones, R. Kern, E. Larson, C. J. Carey, I. Polat, Y. Feng, E. W. Moore, J. VanderPlas, D. Laxalde, J. Perktold, R. Cimrman, I. Henriksen, E. A. Quintero, C. R. Harris, A. M. Archibald, A. H. Ribeiro, F. Pedregosa, P. van Mulbregt, SciPy 1.0 Contributors, SciPy 1.0: Fundamental algorithms for scientific computing in Python. *Nat. Methods* **17**, 261–272 (2020). [doi:10.1038/s41592-019-0686-2](https://doi.org/10.1038/s41592-019-0686-2) [Medline](#)
79. W. McKinney, Data Structures for Statistical Computing in Python. In *Proceedings of the 9th Python in Science Conference* (2010). [doi:10.25080/majora-92bf1922-00a](https://doi.org/10.25080/majora-92bf1922-00a)
80. S. Seabold, J. Perktold, Statsmodels: Econometric and Statistical Modeling with Python. In *Proceedings of the 9th Python in Science Conference* (2010). [doi:10.25080/majora-92bf1922-011](https://doi.org/10.25080/majora-92bf1922-011)
81. J. D. Hunter, Matplotlib: A 2D Graphics Environment. *Comput. Sci. Eng.* **9**, 90–95 (2007). [doi:10.1109/MCSE.2007.55](https://doi.org/10.1109/MCSE.2007.55)
82. T. Oliphant, *Guide to NumPy* (CreateSpace, ed. 2, 2015).
83. M. Parker, seaborn_sinplot; https://github.com/mparker2/seaborn_sinplot.
84. M. Waskom *et al.*, seaborn: v0.5.0 (2014); DOI: 10.5281/zenodo.12710.
85. B. Langmead, S. L. Salzberg, Fast gapped-read alignment with Bowtie 2. *Nat. Methods* **9**, 357–359 (2012). [doi:10.1038/nmeth.1923](https://doi.org/10.1038/nmeth.1923) [Medline](#)
86. P. Danecek, J. K. Bonfield, J. Liddle, J. Marshall, V. Ohan, M. O. Pollard, A. Whitwham, T. Keane, S. A. McCarthy, R. M. Davies, H. Li, Twelve years of SAMtools and BCFtools. *Gigascience* **10**, giab008 (2021). [doi:10.1093/gigascience/giab008](https://doi.org/10.1093/gigascience/giab008) [Medline](#)
87. J. K. Bonfield, J. Marshall, P. Danecek, H. Li, V. Ohan, A. Whitwham, T. Keane, R. M. Davies, HTSlib: C library for reading/writing high-throughput sequencing data. *Gigascience* **10**, giab007 (2021). [doi:10.1093/gigascience/giab007](https://doi.org/10.1093/gigascience/giab007) [Medline](#)
88. G. Dick, *Genomic Approaches in Earth and Environmental Sciences* (Wiley, 2018).
89. N. D. Grubaugh, K. Gangavarapu, J. Quick, N. L. Matteson, J. G. De Jesus, B. J. Main, A. L. Tan, L. M. Paul, D. E. Brackney, S. Grewal, N. Gurfield, K. K. A. Van Rompay, S. Isern, S. F. Michael, L. L. Coffey, N. J. Loman, K. G. Andersen, An amplicon-based sequencing framework for accurately measuring intrahost virus diversity using PrimalSeq and iVar. *Genome Biol.* **20**, 8 (2019). [doi:10.1186/s13059-018-1618-7](https://doi.org/10.1186/s13059-018-1618-7) [Medline](#)
90. K. Katoh, D. M. Standley, MAFFT multiple sequence alignment software version 7: Improvements in performance and usability. *Mol. Biol. Evol.* **30**, 772–780

- (2013). [doi:10.1093/molbev/mst010](https://doi.org/10.1093/molbev/mst010) [Medline](#)
91. B. Goodrich, J. Gabry, I. Ali, S. Brilleman, rstanarm: Bayesian applied regression modeling via Stan (2020); <https://mc-stan.org/rstanarm>.
 92. B. Carpenter, A. Gelman, M. D. Hoffman, D. Lee, B. Goodrich, M. Betancourt, M. Brubaker, J. Guo, P. Li, A. Riddell, Stan: A Probabilistic Programming Language. *J. Stat. Softw.* **76**, (2017). [doi:10.18637/jss.v076.i01](https://doi.org/10.18637/jss.v076.i01)
 93. M. Dowle, A. Srinivasan, data.table: Extension of 'data.frame' (2020).
 94. H. Wickham, *ggplot2: Elegant Graphics for Data Analysis* (Springer, 2016).
 95. O. Tange, GNU Parallel 20201122 ('Biden') (2020); www.gnu.org/software/parallel/.
 96. H. B. Mann, D. R. Whitney, On a Test of Whether one of Two Random Variables is Stochastically Larger than the Other. *Ann. Math. Stat.* **18**, 50–60 (1947). [doi:10.1214/aoms/1177730491](https://doi.org/10.1214/aoms/1177730491)
 97. Additional statistical information and the R code and data to reproduce the results, figures, and tables are available at <https://doi.org/10.5281/zenodo.4774226>.
 98. Y. Furuse, E. Sando, N. Tsuchiya, R. Miyahara, I. Yasuda, Y. K. Ko, M. Saito, K. Morimoto, T. Imamura, Y. Shobugawa, S. Nagata, K. Jindai, T. Imamura, T. Sunagawa, M. Suzuki, H. Nishiura, H. Oshitani, Clusters of Coronavirus Disease in Communities, Japan, January–April 2020. *Emerg. Infect. Dis.* **26**, 2176–2179 (2020). [doi:10.3201/eid2609.202272](https://doi.org/10.3201/eid2609.202272) [Medline](#)
 99. E. H. Y. Lau, G. M. Leung, Reply to: Is presymptomatic spread a major contributor to COVID-19 transmission? *Nat. Med.* **26**, 1534–1535 (2020). [doi:10.1038/s41591-020-1049-3](https://doi.org/10.1038/s41591-020-1049-3) [Medline](#)
 100. A. L. Wyllie, J. Fournier, A. Casanovas-Massana, M. Campbell, M. Tokuyama, P. Vijayakumar, J. L. Warren, B. Geng, M. C. Muenker, A. J. Moore, C. B. F. Vogels, M. E. Petrone, I. M. Ott, P. Lu, A. Venkataraman, A. Lu-Culligan, J. Klein, R. Earnest, M. Simonov, R. Datta, R. Handoko, N. Naushad, L. R. Sewanan, J. Valdez, E. B. White, S. Lapidus, C. C. Kalinich, X. Jiang, D. J. Kim, E. Kudo, M. Linehan, T. Mao, M. Moriyama, J. E. Oh, A. Park, J. Silva, E. Song, T. Takahashi, M. Taura, O.-E. Weizman, P. Wong, Y. Yang, S. Bermejo, C. D. Odio, S. B. Omer, C. S. Dela Cruz, S. Farhadian, R. A. Martinello, A. Iwasaki, N. D. Grubaugh, A. I. Ko, Saliva or Nasopharyngeal Swab Specimens for Detection of SARS-CoV-2. *N. Engl. J. Med.* **383**, 1283–1286 (2020). [doi:10.1056/NEJMc2016359](https://doi.org/10.1056/NEJMc2016359) [Medline](#)
 101. L. Tan, X. Kang, X. Ji, G. Li, Q. Wang, Y. Li, Q. Wang, H. Miao, Validation of Predictors of Disease Severity and Outcomes in COVID-19 Patients: A Descriptive and Retrospective Study. *Med* **1**, 128–138.e3 (2020). [doi:10.1016/j.medj.2020.05.002](https://doi.org/10.1016/j.medj.2020.05.002)
 102. S. Zheng, J. Fan, F. Yu, B. Feng, B. Lou, Q. Zou, G. Xie, S. Lin, R. Wang, X. Yang, W. Chen, Q. Wang, D. Zhang, Y. Liu, R. Gong, Z. Ma, S. Lu, Y. Xiao, Y. Gu, J. Zhang, H. Yao, K. Xu, X. Lu, G. Wei, J. Zhou, Q. Fang, H. Cai, Y. Qiu, J. Sheng, Y. Chen, T. Liang, Viral load dynamics and disease severity in patients infected with SARS-CoV-2 in Zhejiang province, China, January–March 2020: Retrospective cohort study. *BMJ* **369**, m1443 (2020). [doi:10.1136/bmj.m1443](https://doi.org/10.1136/bmj.m1443) [Medline](#)

ACKNOWLEDGMENTS

Computation has been performed on the HPC for Research/Clinic cluster of the Berlin Institute of Health, supported by Dieter Beule, Manuel Holtgrewe, and Oliver Stolpe. Thanks to Udo Gieraths and Leonie Meiners for careful commentary on the manuscript, to the Charité – Universitätsmedizin Pa-COVID-19 collaborative study group for providing additional onset of symptoms data, and to Stephen Kissler for providing additional details regarding their NBA study. The conditions allowing the work to be done with no need for consent are given at <https://gesetze.berlin.de/bsbe/document/jlr-KHGBE2011V4P25> **Funding:** Work at Charité – Universitätsmedizin Institute of Virology is funded by European Commission via project ReCoVer, German Federal Ministry of Education and Research (Bundesministerium für Bildung und Forschung, BMBF) through projects DZIF (301-4-7-01.703) to CD, VARIPath (01KI2021) to VMC, PROVID (FKZ 01KI20160C) to CD, VMC, and LES, and (NaFoUniMedCovid19 (NUM) – COVIM, FKZ: 01KX2021) to CD, VMC, and LES. The Pa-COVID 19 Study is supported by grants from the Berlin Institute of Health (BIH). This study was supported in parts by the German Ministry of

Health (Konsiliarlabor für Coronaviren and SeCoV) to CD and VMC. TCJ is in part funded through NIAID-NIH CEIRS contract HHSN272201400008C. **Author contributions:** TCJ, GB, BM: bioinformatic processing, statistical analysis, interpretation of results, writing original draft and final text; TV: statistical analysis, interpretation of results, writing original draft and final text, next-generation sequencing; JS, JBS, TB, JT, MLS: sample preparation, virus isolation and culturing, RT-PCR, next-generation sequencing; LES, FK: collection of symptom onset data; PM, RS, MZ, JH, AK, AS, AE: diagnostic work and collection of raw data; VMC: diagnostic data collection, viral load calibration, supervision of laboratory work, interpretation of results; CD: project concept, interpretation of results, writing original draft and final text. **Competing interests:** Authors declare that they have no competing interests. **Data and materials availability:** Additional statistical information and the R code and data to reproduce the results, figures, and tables are available (97). This work is licensed under a Creative Commons Attribution 4.0 International (CC BY 4.0) license, which permits unrestricted use, distribution, and reproduction in any medium, provided the original work is properly cited. To view a copy of this license, visit <https://creativecommons.org/licenses/by/4.0/>. This license does not apply to figures/photos/artwork or other content included in the article that is credited to a third party; obtain authorization from the rights holder before using such material.

SUPPLEMENTARY MATERIALS

science.sciencemag.org/cgi/content/full/science.eabi5273/DC1

Supplementary Text

Figs. S1 to S17

Tables S1 to S5

References (98–102)

MDAR Reproducibility Checklist

15 March 2021; accepted 21 May 2021

Published online 25 May 2021

10.1126/science.abi5273

Table 1. Age stratification of first-positive RT-PCR tests and viral load. Column name abbreviations are as follows: N: number of subjects with a positive test result; Pos. %: percentage of positive subjects; Load (sd): mean \log_{10} viral load and standard deviation. ≥ 3 tests: number of subjects with at least three RT-PCR test results, as used in the viral load time course analysis. Age ranges (in years) are open-closed intervals.

Age	All cases				PAMS cases			Hospitalised cases		
	N	Pos. %	Load (sd)	≥ 3 tests	N	Pos. %	Load (sd)	N	Pos. %	Load (sd)
0-5	330	1.8	5.9 (1.84)	16	36	5.1	6.6 (1.87)	32	0.9	5.6 (2.22)
5-10	185	1.8	6.0 (1.73)	12	39	6.2	6.1 (1.83)	18	1.4	5.8 (1.97)
10-15	227	2.2	6.0 (1.76)	8	51	6.9	6.4 (1.92)	22	1.4	6.0 (2.02)
15-20	643	3.0	6.3 (1.87)	39	192	5.1	6.7 (1.77)	121	2.5	6.1 (1.95)
20-25	1637	3.2	6.5 (1.89)	110	696	4.0	6.9 (1.86)	246	2.7	5.9 (1.92)
25-35	4452	3.0	6.6 (1.90)	320	1988	3.9	7.0 (1.83)	614	2.2	6.0 (1.88)
35-45	3393	2.7	6.4 (1.84)	323	1277	3.5	6.9 (1.79)	576	2.0	6.0 (1.90)
45-55	3341	3.1	6.4 (1.81)	401	1012	3.4	6.9 (1.83)	733	2.3	5.9 (1.77)
55-65	3322	2.7	6.3 (1.78)	623	674	3.0	6.8 (1.82)	1039	2.1	5.9 (1.80)
>65	7851	3.0	6.4 (1.79)	2492	145	5.8	6.8 (1.87)	3434	2.3	6.2 (1.86)

Table 2. Pairwise age comparisons of first-positive RT-PCR viral load and estimated culture probability calculated from spline regression or raw data. Only the spline-based regression adjusts for effects of the test center and RT-PCR system. Differences are mean differences, with 90% credible intervals or confidence intervals from null hypothesis significance testing given in parentheses. p MW: p-value from Mann-Whitney *U* test (96).

Sample	Comparison	Spline-based regression (adjusted)		Raw data (unadjusted)	
		Culture probability difference	\log_{10} load difference	\log_{10} load difference	p MW
All	0-5 vs 20-65	-0.067 (-0.167, -0.002)	-0.50 (-0.62, -0.37)	-0.49 (-0.69, -0.29)	<0.001
All	5-10 vs 20-65	-0.054 (-0.132, -0.002)	-0.40 (-0.50, -0.30)	-0.38 (-0.64, -0.13)	0.004
All	10-15 vs 20-65	-0.045 (-0.111, -0.002)	-0.30 (-0.39, -0.22)	-0.42 (-0.65, -0.18)	<0.001
All	15-20 vs 20-65	-0.033 (-0.076, -0.001)	-0.18 (-0.23, -0.12)	-0.16 (-0.31, -0.01)	0.033
PAMS	0-5 vs 20-65	-0.067 (-0.167, -0.002)	-0.50 (-0.62, -0.37)	-0.49 (-0.69, -0.29)	<0.001
PAMS	5-10 vs 20-65	-0.112 (-0.279, -0.003)	-0.63 (-0.96, -0.32)	-0.37 (-1.00, 0.26)	0.213
PAMS	10-15 vs 20-65	-0.092 (-0.228, -0.003)	-0.51 (-0.77, -0.26)	-0.86 (-1.46, -0.26)	0.004
PAMS	15-20 vs 20-65	-0.064 (-0.162, -0.002)	-0.35 (-0.54, -0.17)	-0.56 (-1.10, -0.02)	0.034
Hospitalised	0-5 vs 20-65	-0.033 (-0.087, -0.001)	-0.18 (-0.29, -0.07)	-0.26 (-0.52, -0.01)	0.046
Hospitalised	5-10 vs 20-65	-0.028 (-0.104, 0.009)	-0.18 (-0.45, 0.07)	-0.36 (-1.10, 0.37)	0.115
Hospitalised	10-15 vs 20-65	-0.025 (-0.084, 0.003)	-0.16 (-0.36, 0.03)	-0.48 (-1.38, 0.43)	0.172
Hospitalised	15-20 vs 20-65	-0.022 (-0.071, 0.001)	-0.14 (-0.29, 0.02)	-0.11 (-0.97, 0.74)	0.625
Other	0-5 vs 20-65	-0.018 (-0.055, 0.000)	-0.11 (-0.22, 0.01)	0.00 (-0.33, 0.33)	0.845
Other	5-10 vs 20-65	-0.058 (-0.148, -0.001)	-0.36 (-0.51, -0.20)	-0.33 (-0.55, -0.10)	0.004
Other	10-15 vs 20-65	-0.044 (-0.110, -0.001)	-0.27 (-0.39, -0.15)	-0.10 (-0.40, 0.20)	0.586
Other	15-20 vs 20-65	-0.026 (-0.072, -0.001)	-0.16 (-0.27, -0.06)	-0.31 (-0.58, -0.04)	0.045

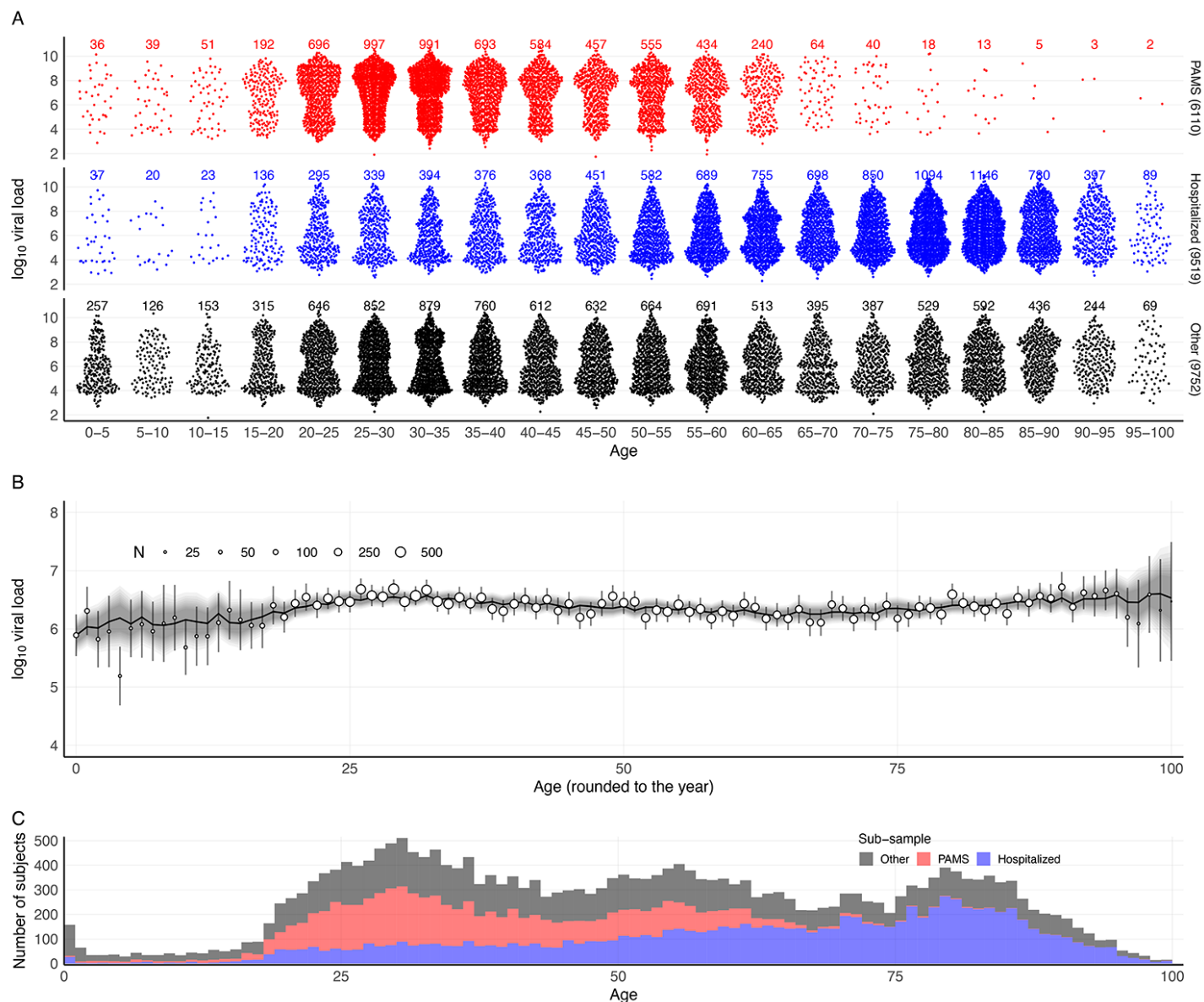


Fig. 1. Distribution of age and first-positive viral load in PAMS, Hospitalised, and Other subjects. (A) Distribution of observed first-positive viral loads for 25,381 subjects according to clinical status (6110 PAMS, 9519 Hospitalised, 9752 Other) and age group. (B) Age-viral load association with observed viral loads and confidence intervals as circles (with size indicating subject count) with vertical lines, and model-predicted viral loads and credible intervals as a black roughly-horizontal line with grey shading. (C) Overlapping age histograms according to subject clinical status. Because inclusion in the study required a positive RT-PCR test result, and testing is in many cases symptom-dependent, the study may have a proportion of PAMS cases that differs from the proportion in the general population.

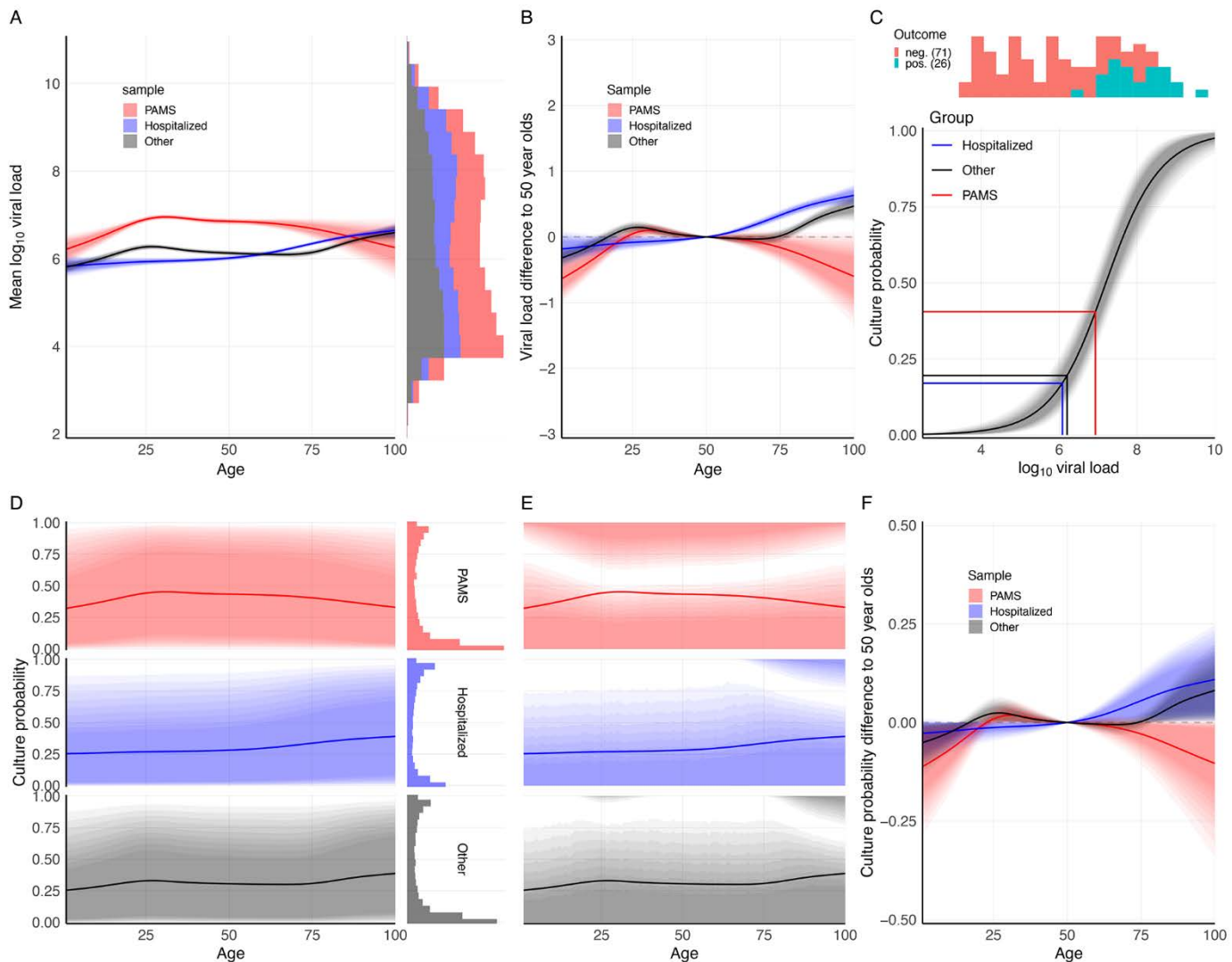


Fig. 2. Estimated viral load and culture probability at time of first positive RT-PCR test. Shaded regions show 90% credible intervals in all panels. To indicate change within each 90% region, shading decreases in intensity from a narrow 50% credibility interval level to the full 90%. **(A)** Estimated mean viral load in first-positive RT-PCR test according to age and status. The stacked histogram (right) shows the observed viral load distribution. Small age-year to age-year variations in the proportion of subjects groups cause the fluctuations in the estimated viral loads for the total sample. Because the shaded region shows the 90% credible interval for the mean, it does not include the higher values shown in the histogram on the right. **(B)** Differences in estimated first-positive viral load according to age and status. Each colored line is specific to a particular subset of subjects (PAMS, Hospitalised, Other). The line shows how viral load differs by age for subjects of the corresponding status from that of 50-year old (rounded age) subjects of the same status. The comparison against those of age 50 avoids comparing any subset of the subjects against a value (such as the overall mean) that is computed in part based on that subset, thereby partially comparing data to itself. The mean first-positive viral load for PAMS and Hospitalised subjects of age 50 are 7.2 and 6.2, respectively, allowing relative y-axis differences to be translated to approximate viral loads. **(C)** Estimation of the association between viral load and cell culture isolation success rate based on data from our own laboratory (19) and the study of Perera *et al.* (20). Viral load differences in the range ~6 to ~9 have a large impact on culture probability, while the impact is negligible for differences outside that range. The vertical lines indicate the observed mean first-positive viral load for different subject groups and the horizontal lines the corresponding expected probability of a positive culture. **(D)** Estimated culture probability at time of first-positive RT-PCR according to age and status, obtained by combining the results in (A) and (C). Culture probability is calculated from posterior predictions, that is the posterior means shown in (A) plus error variance. The histogram on the right shows that mean culture probabilities calculated from observed \log_{10} viral load values are not well-matched by credible intervals, which do not include the most-probable estimated culture probabilities. **(E)** Same y-axis as (D). Culture probability with highest posterior density regions, which do include the most-probable estimated culture probabilities and match the histograms in (D) well. **(F)** Differences of estimated expected culture probability at time of first-positive RT-PCR for age groups, with plot elements as described for (B).

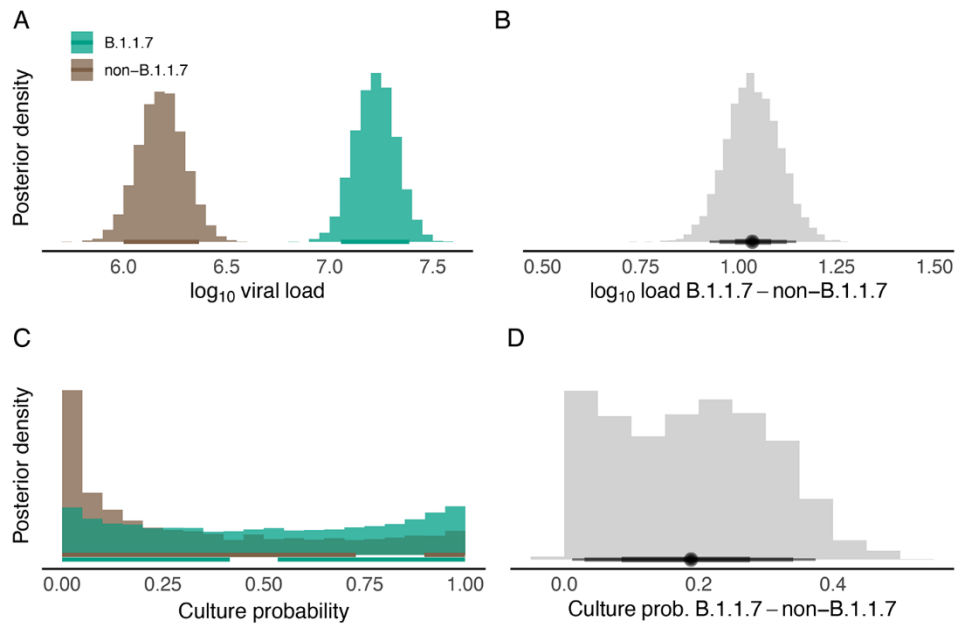


Fig. 3. Posterior distributions of estimated viral loads and culture probabilities for B.1.1.7 and non-B.1.1.7 subjects, and their differences. The viral loads and estimated culture probability of 1387 B.1.1.7 and 977 non-B.1.1.7 subjects. To select a comparable subset of non-B.1.1.7 viral loads for the comparison, non-B.1.1.7 subjects were included only from test centres that had detected a B.1.1.7 variant as well as at least one non-B.1.1.7 subject, and only if the non-B.1.1.7 infection was detected on the same day as a B.1.1.7 infection was detected, plus or minus one day. Similar differences exist when viral loads from larger, less restrictive, subsets of non-B.1.1.7 subjects are used in the comparison (table S2; see materials and methods). (A) Posterior distribution of \log_{10} viral load. (B) Difference of average viral load between B.1.1.7 and non-B.1.1.7 cases. (C) Posterior distribution of the estimated culture probability. See also fig. S2. (D) Difference of mean culture probability between B.1.1.7 and non-B.1.1.7 cases. Horizontal lines in (A), (B), and (D) indicate 90% credible intervals, and the highest posterior density intervals in (C).

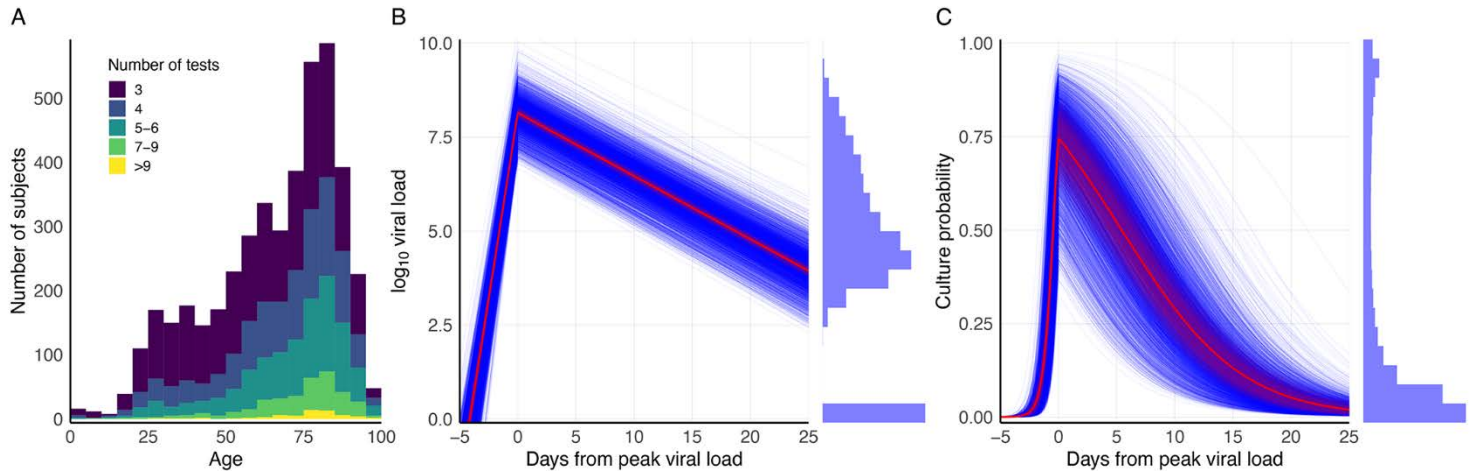


Fig. 4. Viral load and estimated infectious virus shedding time series. Of 25,381 positive subjects, 4344 had three or more RT-PCR test results available and these were used in a viral load time series analysis. Subjects with only one result cannot be placed in time due to inherent ambiguity from the model having both an increasing and a decreasing phase, and those with only two test results were excluded from the time series analysis due to insufficient data for temporal placement (their number of data points is less than number of model parameters being estimated). **(A)** The number of subjects with three or more RT-PCR test results available, at least two of which were positive, according to age. **(B)** Estimated time course of viral load for 18,136 RT-PCR results from the 4344 subjects with at least three RT-PCR results. Blue lines are expected complete time courses for individual cases. The sample mean is shown in red, with its 90% credible interval as a shaded area. The small histogram on the right shows the distribution of all observed viral loads. The histogram values at zero correspond to the initial and trailing negative tests in subject timelines. Raw viral load time series, per subject and split by number of RT-PCR tests, are shown in fig. S8. **(C)** Estimated time course of positive cell culture probability, calculated by applying the results shown in Fig. 2C to the estimated viral load time courses in (B). Blue lines are expected time courses for individual subjects. The sample average is shown in red, with its 90% credible interval as a shaded area. The small histogram to the right shows the distribution of culture probability in the sample, and was obtained by applying the curve in Fig. 2C to the data in the histogram in (B).

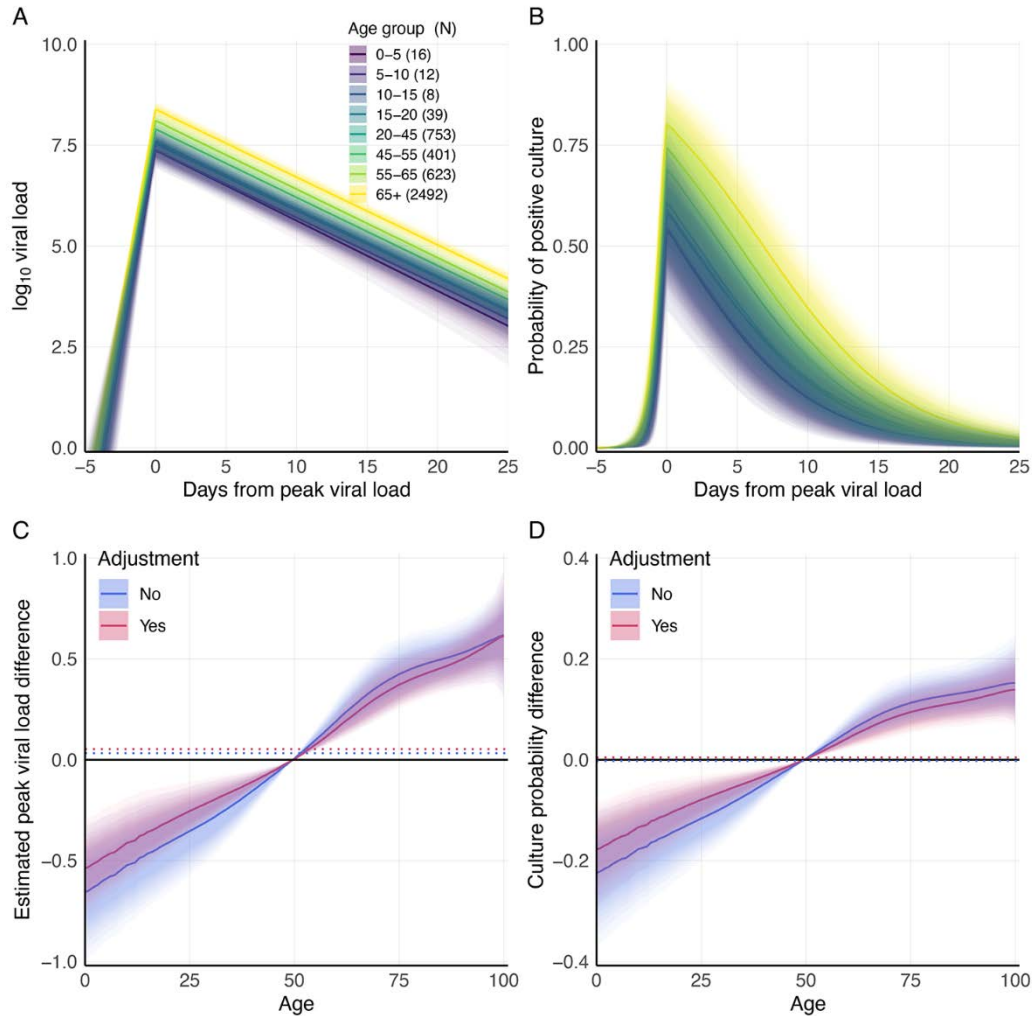


Fig. 5. Estimated expected viral load and culture probability for age groups by time. (A) Change in estimated viral load over time according to age group for 4344 subjects with at least three RT-PCR tests, at least two of which were positive. The age coloring, range, and number of subjects in each category is given in the figure legend. Shading indicates the 90% credible interval of the mean. (B) Change in estimated culture probability over time according to age. Age groups, coloring, and shading are as in (A). (C) Estimated age group differences in mean peak viral load, corresponding to the values at day zero in (A). (D) Estimated age group differences in mean peak culture probability, corresponding to the values at day zero in (B). In (C) and (D), adjusted differences account for variations by age in clinical status and gender.

Estimating infectiousness throughout SARS-CoV-2 infection course

Terry C. Jones, Guido Biele, Barbara Mühlemann, Talitha Veith, Julia Schneider, Jörn Beheim-Schwarzbach, Tobias Bleicker, Julia Tesch, Marie Luisa Schmidt, Leif Erik Sander, Florian Kurth, Peter Menzel, Rolf Schwarzer, Marta Zuchowski, Jörg Hofmann, Andi Krumbholz, Angela Stein, Anke Edelmann, Victor Max Corman and Christian Drosten

published online May 25, 2021

ARTICLE TOOLS

<http://science.sciencemag.org/content/early/2021/05/24/science.abi5273>

SUPPLEMENTARY MATERIALS

<http://science.sciencemag.org/content/suppl/2021/05/24/science.abi5273.DC1>

REFERENCES

This article cites 86 articles, 10 of which you can access for free
<http://science.sciencemag.org/content/early/2021/05/24/science.abi5273#BIBL>

PERMISSIONS

<http://www.sciencemag.org/help/reprints-and-permissions>

Use of this article is subject to the [Terms of Service](#)

Science (print ISSN 0036-8075; online ISSN 1095-9203) is published by the American Association for the Advancement of Science, 1200 New York Avenue NW, Washington, DC 20005. The title *Science* is a registered trademark of AAAS.

Copyright © 2021 The Authors, some rights reserved; exclusive licensee American Association for the Advancement of Science. No claim to original U.S. Government Works. Distributed under a Creative Commons Attribution License 4.0 (CC BY).